A STUDY OF THE RADIATION PROCESS OF PULSARS

By

DAVID JAMES GORDON

Bachelor of Arts
Marist College
Poughkeepsie, New York
1971

Master of Arts
State University of New York, College at New Paltz
New Paltz, New York
1974

Submitted to the Faculty of the Graduate College
of the Oklahoma State University
in partial fulfillment of the requirements
for the Degree of
DOCTOR OF PHILOSOPHY
July, 1982

A STUDY OF THE RADIATION PROCESS OF PULSARS

Thesis Approved:

N. V. V. J. Swamy
Thesis Adviser

Larry E. Hallidmton

Leon W. Schmeder

Norman N Durham
Dean of the Graduate College

TO MY TEACHERS

David and Dorothy Gordon

Frank Ebelheiser

Leonard Zimet

Robert Pease

Paul Westhaus

PREFACE

This study is an attempt to fill in some gaps in the theory of pulsar radiation as it stands today. At the present time progress in understanding the source of the radiation seems to be stalled. In developing this thesis a number of ideas were generated dealing with precession of the pulsar, correlation of circular polarization with the height of the region in which the radiation is generated and the contribution of the supersonic aspect of the plasma to the production of shock fronts.

In the present work radiation by linear acceleration of charge, radiative transfer through a plasma traveling at relativistic speeds and shock waves in a supersonic plasma were studied. We have tried to add to the present knowledge in each of these areas. Work in each of these areas has suggested further refinements which might make the results agree more closely with observations.

I would like to express my appreciation to Dr. N. V. V. J. Swamy for serving as my adviser and for his contribution to the chapter on shocks in supersonic flow. I would also like to thank Dr. Larry Halliburton, Dr. Leon Schroeder, Dr. Larry Scott and Dr. Rao Yarlagadda for serving on my committee.

I would also like to make note of my friend and fellow traveler Weldon Wilson with whom I started out together with on this course of study in physics. He has provided a good mind and a degree of expertise for our discussions. I would like to thank Ms. Janet Sallee for typing this work in her normal excellent style. In addition I would like to

thank the Department of Physics at Oklahoma State University, Phillips Petroleum, and the people of the State of Oklahoma for providing the funds in the form of various research and teaching positions to support me during my course of study.

All in all I find this kind of work quite enjoyable and I look forward to more of the same.

TABLE OF CONTENTS

Chapter		Page
I.	INTRODUCTION.	1
	Model Pulsar	2
	Study Outline.	12
II.	RADIATION CHARACTERISTICS	17
	Integrated Pulse Observations.	20
	Single Pulse Characteristics	24
	Summary.	28
III.	RADIATION MECHANISM THEORIES AND A CALCULATION FOR THE SPECTRUM OF A LINEARLY ACCELERATED CHARGE	31
	Radiation Mechanisms	32
	Equation of Motion for Linearly Accelerated Charge .	38
	Retarded Radiation Fields and Their Spectral Analysis.	42
	Results.	47
IV.	RADIATIVE TRANSFER.	56
	Dispersion Relations	57
	Hartree-Appleton Equation.	60
	Relativistic Treatment of Dispersion Relations . . .	67
	Summary.	81
V.	RADIATION COHERENCE AND PLASMA SHOCKS	84
	Theory of Shocks	85
	Jump Conditions for a Moving Shock	91
VI.	SUMMARY AND CONCLUSIONS	95
A SELECTED BIBLIOGRAPHY		98
APPENDIX.	FUNCTION GENERATION AND THE FAST FOURIER TRANSFORM PROGRAM.	99

LIST OF FIGURES

Figure		Page
1.	Log-Log Plot of Differential Intensity Vs. Frequency. . . .	48
2.	Radiation Pattern for Linearly Accelerated Charge	49
3.	Determinant for Calculating the Dispersion Relation	76
4.	Energy-Momentum Tensor θ_{ik} and Electromagnetic Energy-Momentum Tensor S_{ik}	88
5.	Lorentz Transformation of Total Stress-Energy Tensor. . . .	89

CHAPTER I

INTRODUCTION

Pulsars are a class of astronomical objects which emit intense, short duration, periodic pulses of electromagnetic energy primarily in the radio frequency spectrum. They were first discovered by Bell-Burnell in 1967 while working with a team under Hewish studying scintillations by the solar wind.[1] In the fourteen years since then these objects have been at the focus of a great deal of study in an attempt to explain their nature. Although at the present time there is agreement regarding the broader aspects of pulsar construction and operation, attempts to fill in the details have yet to produce a model upon which researchers can agree. One aspect of the model pulsar which has been worked on extensively, although without producing a clearcut theory, is the manner in which the observed radiation is produced.[2] Knowledge of the radiation mechanism is of obvious importance to the understanding of the nature of pulsars. The purpose of this work is to study some of the possible aspects of the radiation mechanism of pulsars which have not been closely examined by others.

For this introductory section of our study we will first discuss those aspects of pulsar theory which are accepted by most researchers. This model pulsar is the starting point for more detailed models.

Model Pulsar

The development of the model pulsar proceeded in large part by the process of elimination. The sky is full of objects whose periodic fluctuations in intensity have been well studied and successfully explained. What was needed was an object which could produce intensity variations at intervals between 0.03 and 4 seconds with a stability of 1 part in 10^8 over a period of several months and a pulse duration of about 10% of the pulse period.[3] The stability of the pulse period demanded that the mechanism producing it be the conservation of angular momentum of a very massive body.[4] This meant that either eclipsing binary systems or rotating stars were the source of the pulses. Physically pulsating stars were discarded since the pulse durations were short enough to demand expansion and contraction speeds beyond what were possible for a stable star. Also stars pulsating at this rate would radiate energy through gravity waves and thereby slow down at a greater rate than was observed.[5] Eclipsing binary star systems would require orbits with semi-major axes less than 10^5 km ($R_{moon} = 3.85 \times 10^5$ km). This lies within the Roche limit and the tidal forces would destroy the components of the system.[6] Furthermore when the resolution on the pulses was improved they exhibited structure which would be very difficult to explain with an eclipsing binary system model. This left rotating stars with the radiation associated with a small area on its surface as the only possible candidate. The only star types which had sufficiently strong gravitational fields to hold them together at the observed high angular velocities were white dwarfs and neutron stars. When pulsars with periods shorter than 0.1 second were discovered the white dwarfs were also eliminated leaving neutron stars as the only possible choice.[7]

At that time neutron stars were hypothetical objects which had been first introduced by Baade and Zwicky in 1934 as the end product of a supernova explosion, the final stage of stellar evolution for very massive stars.[8] In a supernova explosion the core of a star undergoes a gravitational collapse in which electrons and protons react to become neutrons. In the course of this collapse the energy which is released violently blows off the mass surrounding the core producing an expanding cloud of gas or a nebula. If the core of the star has a mass that is less than 2-3 solar masses, then the energy of the neutrons in their degenerate state is believed to be sufficient to halt the gravitational collapse. The remnant becomes a rapidly rotating body composed primarily of neutrons. Calculations of the Oppenheimer-Volkoff equation, the equation of state, for this nuclear matter have shown that the star will be stable with a mass between 1 and 2 solar masses and a radius of 10 km.[9] The increase in rotational speed ($\Omega_{sun} = 2.7 \times 10^{-6}$ rad/sec., $\Omega_{pulsar} = 10^{2}$ rad/sec.) is due to the conservation of angular momentum. The fact that two pulsars have been discovered in nebulae associated with supernova explosions lends support to the choice of neutron stars as being responsible for pulsars.[10,11]

The next step in constructing the model pulsar was to learn the cause of the intense pulses of radiation. Since the star no longer has a nuclear energy source its surface temperature decreases and it loses luminosity. Pre-pulsar neutron star searches consisted in looking for X-ray sources in nebulae associated with supernovae. It was thought that charged matter falling into the star would be accelerated by the large gravitational fields to the extent that it would emit X-rays. This method is still used to search for black holes and the mechanism is used

to explain X-ray pulsars.[12] The radiation from pulsars is extremely intense. If the source were emitting incoherent radiation the temperature would have to be of the order of 10^{30} K.[13] Since this temperature is unrealistic the radiation from the pulsar must be coherent.

It had long been suspected that when a star collapsed the magnetic flux of the star was compressed, greatly increasing the star's field strength. This is fairly well established by the freezing-in theory of plasma physics. Since the dipole field is proportional to the inverse cube of the distance from the magnetic moment a reduction in stellar radius from 10^5 km to 10 km, a reduction by 10^4, meant that the field at the pole would increase by a factor of 10^{12}. For typical fields of 1 Gauss this meant that the surface field of a pulsar could be of the order of 10^{12} Gauss, perhaps the strongest magnetic field in the universe. Interestingly enough several months prior to the discovery of the first pulsar Pacini suggested that a neutron star with a rotational period of 0.01 seconds and a magnetic field strength of 10^{12} G was the source of energy for the expansions and the synchrotron radiation observed in the Crab Nebula.[14] Within a year the pulsar was found with a period of 0.033 second.[15]

Several months after the discovery of the first pulsar Gold made the suggestion that the radiation pulses were asssociated with the intense magnetic field.[16] He noted that the fields were strong enough to cause charged particles to corotate with the star. This corotation would cause charges at a distance of $\frac{c\,T}{2\pi}$ from the axis of rotation of a pulsar with rotational period of T to travel at the speed of light, c. This distance from the axis has come to be known as the radius of the light cylinder. Although the charges do not reach the speed of light,

they do become highly relativistic. Charges traveling at these speeds could then radiate for a number of relativistic reasons. Unfortunately the gravitational field of a neutron star which is 10^8 times stronger than the Earth's will only allow an atmosphere a few centimeters in height according to the normal barometer formula.[17] This problem was addressed by Goldreich and Julian in 1969 when they noted that there was a mechanism available which could provide a neutron star with an extensive atmosphere of charged particles.[18] It had been known for some time that rotating conductors with embedded magnetic fields would produce electric fields about them in a process known as unipolar induction. Goldreich and Julian pointed out that the interior of a neutron star was an excellent conductor and that the same process should occur there. The effect is due to the Lorentz force on the charges within the star. If the charges are considered inertialess in the first approximation they will distribute themselves in such a manner that the electric field they produce negates the induction field. This field would be given by

$$\vec{E} = -\frac{1}{c}(\vec{\Omega} \times \vec{r}) \times \vec{B}$$

where Ω is the angular velocity. If we assume the magnetic moment is aligned with the angular velocity vector and that the field is due to a dipole at the center of the star, the external field becomes

$$\vec{E} = \frac{B\Omega R^5}{c\, r^5}(P_2(\cos\theta)\hat{r} + \sin\theta\cos\theta\,\hat{\theta}) \ .$$

At the poles of the star $B = 10^{12}$ G, R = radius of the star = 10^6 cm = r, and Ω = angular velocity is typically 10 rad/sec. The field in this case would be of the order of 10^9 V/cm which exceeds the gravitational

force by a factor of 10^{12} for electrons and 10^{9} for protons.[19] The charges would then be expected to leave the surface of the star following the strong magnetic field lines to produce an atmosphere of corotating plasma about the star. This argument ignores the magnitude of the work function for removing the charges from the surface. It is felt, however, that the electrons would move freely from the surface into the atmosphere and the ions would not be sufficiently bound to prevent them from escaping. In 1971 Mestel, Cohen and Toton proved that this magnetosphere would be produced even if the magnetic moment was perpendicular to the rotational axis.[20,21]

The discovery of this magnetosphere about the neutron star was of great importance in understanding the radiation from pulsars. The magnetosphere contains charged separated plasma, very strong electric and magnetic fields, and charges moving at speeds close to the speed of light. These ingredients would seem to be too adequate for producing the intense radiation which is observed. The problem then is in finding the configuration of the fields and currents which exist in the magnetosphere. To date no closed form solution has been found. Since the magnetosphere is central to developing a radiation mechanism we will review some of the aspects of current models.

Magnetosphere

Considering that we still have no complete understanding of the magnetosphere of the sun it comes as no surprise that the magnetosphere about a pulsar is even less understood. There is some common ground for the different theories which have been advanced. First is the idea of charge separated plasmas in the magnetosphere. In the case of aligned

magnetic moment and rotational axis the electric field lines run from the equatorial region to the polar caps. We would therefore expect electrons to be emitted from the surface of the star at the higher latitudes and protons to be emitted at the lower latitudes.[22] In the absence of magnetic fields we would get currents flowing between the two regions. The very strong magnetic fields alter this situation. With fields of the order of 10^{12} G any motion perpendicular to the field will cause the particles to spiral about the field lines. Since the dipole configuration of the magnetic field is not similar to the quadrapole configuration of electric field their field lines will cross so that the magnetic field will inhibit the current flow.

The regions close to the poles of the star will have a special significance. The magnetic field lines will corotate with the star. This means that lines which originate from the polar zones will extend through what is known as the light cylinder. This is an imaginary cylinder enclosing the star whose radius is equal to $\frac{c\,T}{2\pi}$ and whose axis is parallel to the stars rotational axis. Its significance is that any point beyond this cylinder which corotates with the star must move faster than the speed of light. When charges leave the surface of the star they are forced to follow the magnetic field lines. If they are emitted along lines originating from the polar regions they will travel to the light cylinder and reach relativistic speeds. At this point it is suspected that due to a relativistic change in inertia the charges will alter the shape of the dipole configuration of the field causing the magnetic field lines to be open.[23] This gives the charges a route to escape from the star and raises the possibility of a continuous current flow from the polar regions.. The surface of the star where these

charges originate is divided into two zones. The higher latitudes, where the field lines terminate, is referred to as the electron polar zone and the lower latitudes where the field lines originate is called the proton polar zone.[24] The names derive from the particles which are emitted there. The particles above these regions are thought to be charge separated due to the outward current and the loss of charge along the open field lines. This is an important point since it allows for concentrations of charge which could help explain the intensity of the radiation.

It is important to bear in mind that the foregoing relates to the simplified case where the magnetic moment and rotational axis were aligned. The more realistic case where the two are at an inclination will start have open field lines but the geometry of the polar zones will be more complicated.[25]

The density of particles in the regions above these zones has been estimated to be of the order of 10^{8} - 10^{12} cm^{-3} by using estimates of mass loss in the Crab Nebula and by treating the corotating magnetosphere as an extension of the star and calculating the charge distribution due to induction effects.[26]

A second important feature of the magnetosphere is its enormous field strengths. As has been noted, the magnetic field strength is quite important in determining the current flow in the magnetosphere. It has also been noted that in the case where the star is surrounded by a vacuum the electric fields may be of the order of 10^{12} V/cm. What actually happens is that charges leave the surface of the star along the field lines and distribute themselves in such a manner so as to reduce this field. How the fields are rearranged due to this charge redistri-

bution and the current flow is the main problem concerning the researchers dealing with the magnetosphere. It is fairly certain however that extremely large electric fields do exist in the magnetosphere, whether close to the surface or to the light cylinder.

A third point to be noted is that the magnetosphere is a relativistic plasma in the sense that it has bulk velocities approaching the speed of light. These speeds are due to the corotation of the magnetosphere and also the large accelerating potentials which may produce electron energies of the order of 10^{12} eV.[27] This relativistic aspect of the plasma has been used in diverse models to explain the beaming effect of the radiation from regions near the light cylinder and the production of curvature radiation from currents traveling along the magnetic field lines near the surface of the star. The relativistic aspect of the plasma offers a number of possible mechanisms to produce radiation such as synchrotron radiation, Cerenkov radiation, and radiation due to the linear acceleration of charges.

The characteristics given above are fairly well accepted and are incorporated in most models of pulsar magnetospheres. The development of more detailed models is usually done in conjunction with the study of a radiation mechanism. This connection will be discussed in a later section of this study. Here we will review the development of some of the model pulsar magnetospheres.

Although the problem may be set up mathematically, its non-linear formulation is not currently solvable. This means that techniques of simplification and non-linearization have been employed to make any headway towards a solution. The first simplification was to assume inertialess particles in the magnetosphere so that they will distribute them-

selves to give zero electric field parallel to the magnetic field, i.e. $\vec{E} \cdot \vec{B} = 0$. Then the equations are solved using an iterative technique to give a self-consistent solution. Solutions of this type show that there would be corotation of the magnetosphere.[28] If currents are introduced along the open field lines it was shown that they would produce a toroidal field about the star and that points of zero field would be produced near the light cylinder. It is expected that charges might accumulate at these null points and possibly play a role in the radiation mechanism.[29] Works by Scharlemann, Henderson and Norton have shown that the acceleration of charges could take place by a centrifugal force sling action or a radiation pressure surfing type action in regions within and outside the light cylinder respectively.[30,31] Since large amounts of current flow along the open field lines escaping from the star, the $\vec{E} \cdot \vec{B} = 0$ approximation is not thought to be very good.

Works which attempt to take these parallel electric fields into account are forced by the complexity of the problem to deal with localized regions of interest and make assumptions concerning the effects that other regions would have there. The region most often dealt with is that which is above the polar zone where the open field lines originate.

The calculations of most interest consist of finding the electric field strength and the current density. Sturrock was first to attempt this by assuming that the potential available was equal to the potential drop across the extremes of the polar zone on the surface of the star.[32] This gave a potential drop of 10^{12} V which produced electrons with a relativistic factor $\gamma = 10^{7}$. He assumed that the electrons traveling along the magnetic field lines would emit curvature radiation due to

their acceleration. This radiation in turn would produce electron positron pairs. According to Sturrock fluxes of 10^{40} particles/sec would be produced through a cascade action and flow into the nebula surrounding the Crab Pulsar. This calculation is really an upper limit since it unrealistically uses the full potential drop across the polar zone.[33] Michel made the calculation taking into account a more reasonable potential drop across the polar zone and has shown that it would be equal to 5×10^{9} V giving a relativistic factor of 10^{4}.[34]

Rudermann and Sutherland treated the case where the ions would be bound too tightly to be emitted from the surface.[35] According to their treatment charge flow would be cut off as the preferential flow of electrons built up a positive charge on the surface of the star. In regions above the polar zone a vacuum gap would be formed in which large electric fields would exist. These gaps would grow until the potential across them reached 10^{12} V at which time sparking would occur due to the formation of electron-positron pairs. The electrons would be accelerated towards the surface of the star producing curvature radiation and the positrons would be accelerated outward producing cascades of particles in a manner similar to that suggested by Sturrock. The calculation showed that the relativistic factor for the escaping positrons would be $\Upsilon = 10^{3}$ and the density of the secondary particles would be given by

$$n = 5 \times 10^{13} \times \left(\frac{R}{r}\right)^{3} \text{ cm}^{-3} .$$

Here the stars radius is R and the density goes as r^{-3} due to the form of the dipole field.

Another region of the magnetosphere which has been of interest is that near the light cylinder. The relativistic characteristics of the

plasma in that region make it of particular interest in determining its radiation capabilities. Of importance is the determination of the relativistic factor of the plasma. Henriksen pointed out that the speed of the corotating plasma could not exceed the speed of propagation of electromagnetic disturbances, the Alfven velocity.[36] For conditions which exist in the magnetosphere this gives a typical relativistic factor $\gamma = \sqrt{2}$. This is an upper bound and an analysis by Hinata and Jackson shows a more realistic value to be only mildly relativistic with the the velocity factor $v/c = .05$.[37] This analysis puts restrictions on the corotating regions' ability to beam radiation relativistically, as has been suggested.[38]

Although the models presented to date do not give an unambiguous account of the magnetosphere configuration they do suggest certain processes which may be occurring there and set limits on the parameters of interest such as particle density and electric field intensity. It is these aspects of the theory which are of interest to us in formulating a radiation mechanism.

Study Outline

In this study we will attempt to contribute to the theory pertaining to pulsar radiation mechanisms. In the first part we will look at the observations which have been made of the radiation. Hints to the processes contributing to the production of the radiation must be contained in the characteristics of the signals. As will be seen, the radiation is quite complicated and the various characteristics and their interrelationships should help us to understand their origin. Next we will look at the simplest method of producing the radiation, that of linear accel-

eration. Although this mechanism has been previously suggested little has been done with it due to a lack of knowledge of the spectrum it produces. In this section we will calculate the spectrum and show that certain aspects of it are in agreement with observation. The fourth part of this work deals with the radiative transfer of the electromagnetic energy through the plasma. Since the problem is relativistic in nature we first review the non-relativistic theory as a starting point and a check for our results. We then calculate the dispersion relation for conditions expected in the region of emission and show that the low frequency cutoff observed in the spectra of some pulsars may be due to the plasma. In the last section we look at the manner in which shock waves travel through the plasma. This is important since localizations of charge whose dimensions are smaller than the wavelength of the radiation which is emitted are capable of producing coherent radiation.

FOOTNOTES

[1]A. Hewish, S. J. Bell, J. H. D. Pilkington, P. F. Scott, and R. A. Collins, Nature 217, 709 (1968).

[2]F. C. Michel, Rev. Mod. Phys. 54, 1 (1982).

[3]T. Gold, Nature 218, 731 (1968).

[4]Ibid.

[5]K. Thorne, Astrophys. Jour. 158, 1 (1968).

[6]J. P. Ostricker, Nature 217, 1127 (1968).

[7]T. Gold, 731.

[8]W. Baade and F. Zwicky, Proc. Nat. Acad. Sci. 20, 254 (1934).

[9]J. R. Oppenheimer and G. Volkoff, Phys. Rev. 55, 374 (1939).

[10]M. I. Large, B. Y. Mills and A. E. Vaughn, Nature 220, 340 (1968).

[11]D. H. Staelin and E. C. Reifenstein, Science 162, 1481 (1968).

[12]Ya. B. Zeldovich and O. K. Guseynov, Astrophys. Jour. 144, 840 (1965).

[13]R. N. Manchester and J. H. Taylor, Pulsars (W. H. Freeman and Co., San Francisco, 1977), p. 7; probably the best book in print on the subject.

[14]F. Pacini, Nature 216, 567 (1968).

[15]M. I. Large, et al., 340.

[16]T. Gold, 731.

[17]F. Hoyle, J. V. Narliker and J. Wheeler, Nature 203, 914 (1964).

[18]P. Goldreich and W. H. Julian, Astrophys. Jour. 157, 869 (1969).

[19]F. G. Smith, Pulsars (Cambridge University Press, Cambridge, 1977) pp. 47, 48.

[20]J. M. Cohen and E. T. Toten, Astrophys. Let. 7, 213 (1971).

[21]L. Mestel, Nature Phys. Sci. 233, 149 (1971).

[22]P. A. Sturrock, Astrophys. Jour. 164, 529 (1971).

[23]P. Goldreich and W. H. Julian, 869.

[24]P. A. Sturrock, 529.

[25]Ibid.

[26]P. Goldreich and W. H. Julian, 869.

[27]Ibid.

[28]E. T. Scharlemann, R. V. Wagnoner, Astrophys. Jour. 182, 951 (1973).

[29]F. C. Michel, Astrophys. Jour. 180, 207 (1973).

[30]E. T. Scharlemann, Astrophys. Jour. 193, 217 (1974).

[31]J. A. Norton and R. N. Henrikson, Astrophys. Jour. 201, 431 (1975).

[32]P. A. Sturrock, 529.

[33]E. Tademaru, Astrophys. and Space Sci. 30, 179 (1974).

[34]F. C. Michel, Astrophys. Jour. 192, 713 (1974).

[35]M. A. Rudermann and P. G. Sutherland, Astrophys. Jour. 196, 51 (1975).

[36]R. N. Henrikson and D. R. Rayburn, Mon. Not. Roy. Astron. Soc. 166, 409 (1974).

[37]S. Hinata and E. A. Jackson, Astrophys. Jour. 192, 703 (1974).

[38]F. G. Smith, Mon. Not. Roy. Astron. Soc. 149, 1 (1970).

CHAPTER II

RADIATION CHARACTERISTICS

In order to understand the manner in which the radiation is produced it is necessary to make a careful study of the characteristics of the pulsar's signal. In this section we will review the techniques used to observe the radiation, as well as their limitations, and look at the common traits among the pulsar emissions. These traits are of obvious importance to developing a theory of pulsar emission. On the other hand exceptions to these common traits must also be taken into account by the theory.

Pulsars are difficult to detect. This is due mainly to the low intensity of their signals; the strongest of which have flux densities of less than 1 Jansky (1 Jansky = 10^{-26} $W\text{-}m^{-2}\text{-}Hz^{-1}$). This signal strength is at the lower limit of pre-pulsar observational technique. Because of the weak signals only the largest radio telescopes are capable of making the searches. Out of 150 pulsars 110 were discovered by the large telescopes at the observatories at Aricebo, Puerto Rico, Jodrell Bank, England, and Molonglo in Australia. Prior to the discovery of pulsars, weak sources were detected by integrating or taking time exposures of the signals. If the integration time was longer than the pulse period, this method would, of course, be useless for detecting pulsed sources. Since weak signal techniques meant long integration times, the receivers used in radio astronomy had long response times which were of the order

of the pulse period or longer. This also tended to wash out any evidence of pulsed emission. When Hewish's group set up their equipment to study the solar wind scintillations of quasar radiation, they needed very sensitive receiver-antenna combinations with a time resolution of 0.1 second. This was one of the first times this combination of apparatus was used in radio astronomy. With signals this weak the system noise becomes the limiting factor. The first source of thermal noise is the antenna structure which produces a signal strength of

$$W_{NA} = k T_A \Delta\nu .$$

For typical values of antenna temperature $T_A = 290^{o}K$ a bandwidth of $\Delta\nu = 10^{6}$ Hz and Boltzmanns constant being $k = 1.38 \times 10^{-23}$ J-K^{-1} we have $W_{NA} = 4 \times 10^{-25}$ W. For an antenna such as the 250 ft device at Jodrell Bank this would correspond to a signal of 25 Janskies. The receivers also have their own noise although they are operated at a much lower temperature to reduce this factor. Typically they are operated at $100^{o}K$. A noise figure from such a system may be up to the order of 100 Janskies. Another limiting characteristic of the system is the sensitivity of the receiver. The sensitivity is proportional to the square root of the product of its bandwidth and the integration time. For signals with durations of 10^{-2} second and receivers with a bandwidth of 1 MHz this gives a sensitivity which is a factor of 100 better than the noise figure. This means that the system above could only detect the strongest pulsars.

Two aspects of pulsar radiation work against the radio astronomer. First is that the integration time must be short enough to detect the pulsed aspect of the radiation. Second is that the dispersion of the

signal limits the usable bandwidth. A reduction of either of these decreases the sensitivity of the receiver.

Signals through a tenuous plasma will have a frequency dependent group velocity i.e., they will be dispersed. If the pulsar is a distance L from the observer and the density of the plasma in the intervening space is N then the travel time of the pulsars signal is

$$t = \frac{L}{v_g} = \frac{N r_o c \nu^{-2} L}{2\pi} = 1.35 \times 10^{-3} \nu^{-2} NL$$

where r_o is the classical electron radius e^2/mc^2 and ν is the frequency of the signal.[1] The product N·L is referred to as the dispersion measure and is given the units of parsec/cm^3. It is a measure of the spread of the signal. This dispersion causes a smearing of the signal which reduces the intensity since all frequencies are not received at the same time. Since the dispersion is proportional to the distance to the pulsar the effect will limit the distance out to which pulsars may be detected. It also provides a method for measuring the distance to pulsars if an average density of interstellar matter is assumed.

In order to increase the sensitivity of a search procedure a process known as de-chirping is applied to the signal. The receivers bandwidth is divided into a number of channels. Each channel is then run through a delay line of increasing delay. The signal is then recombined by adding the signals. By running the channels of progressively higher frequencies through longer delays the process in effect acts to de-disperse the signal. Since there is no prior knowledge of the signal dispersion in a search situation, the delays must be programmed to sweep through a range so as to look at all possible dispersions. With the emergence of digital

techniques this process has become easier to implement. The first dechirpers were 20 channel mechanical affairs.[2] The procedure is also used when it is desirable to get better resolution so as to study the shape of the pulse and the spectrum. In the case of the pulsar in the Crab Nebula the dispersion causes the signal to smear over a bandwidth of 100 KHz.

The most successful procedure for identifying weak pulsars is to Fourier analyze the incoming signal and look for frequency components between .1 and 50 Hz. The signal is typically divided into 12,000 segments each .02 second in length and digitized. The data are then analyzed with a fast Fourier transform while the next data segment is being received.

Once a pulsar is found a variety of measurements are made to determine its characteristics. These measurements are made in two time regimes. One method uses the repetitiveness of the signal to get a period average of the incoming signal. This technique stacks from 200 to 500 pulse periods and adds them to give an integrated pulse profile while at the same time reducing the noise. The other method studies the individual pulses. This technique may only be used for the stronger pulsar signals. Zheleznyakov compares the two regimes to observing the climate and the weather of the radiating region.[3]

Integrated Pulse Observations

The characteristics of the integrated pulse are the easiest to observe since by their nature the energy may be collected over hundreds of pulses. These signals are characterized by the integrated pulse profile or shape. The two classifications are simple pulses where the

pulse consist of only one peak and complex pulses where the profile has more than one peak. The integrated pulse profile is extremely stable. The one exception to this is the mode changing pulsar where there are two stable modes which switch back and forth with one of the modes being dominant. A subclassification for pulse profiles comes from the observation of individual pulses. In a number of cases the integrated profile is built up from individual pulses which drift across the profile in a regular manner. These pulsars are referred to as drifting (D). Both the simple (S) and complex (C) pulses may have this attribute. The pulse profiles are usually between 3 and 5% of the pulse profile in width at half pulse energy although some may be as wide as 21%, e.g., PSR 1911 + 03, P = 2.33s.[4] A few pulsars display an interpulse separated by approximately half a pulse period from the main pulse. The interpulse energy varies from 1 to 85 percent of the main pulse's energy.

There seems to be no correlation of the pulse width and the pulse period. The complex pulse profiles usually consist of two peaks although in some cases up to five peaks have been observed. The relative intensity of the peaks is usually different. There seems to be no preference for the position of the dominant peak. Both the width of the simple pulses and the separation of the pulse components of the complex pulses seem to have a frequency dependence. This dependence is characterized by a power law

$$\Delta\phi = \nu^{p}$$

where Δc is the pulse separation and p is the separation index. For most pulsars p is typically -.2 at the low frequencies.[5] This has an effect of decreasing the pulse separations as the frequency increases.

Most pulsars show a change in the separation index at higher frequencies in which the index becomes more positive, sometimes becoming positive so as to give an increase in separation of the peaks with increasing frequency. The width of the individual peaks is also frequency dependent with a negative power law. Typically the width at 4.9 GHz is 15% narrower than the peak at 2.7 GHz.[6]

The observed energy in the integrated pulse varies both spectrally and temporally. As we will see, individual pulses vary from 0 to 1000 percent of the mean pulse energy. Pulses integrated over 200 to 500 periods have energies which are constant over a period of a few hours but may vary as much as a factor of two over the course of a day and by as much as an order of magnitude over the course of a month. Because of this great variation in magnitude, spectral measurements must be made simultaneously at all frequencies to have any validity. Since many features of pulsar radiation are frequency dependent, for comparison purposes most measurements are made at 400 MHz when possible.

Spectral measurements of pulsars show them to be broadbanded from 100 MHz to 10 GHz. Measurements show little structure and the spectra of pulsars is given by a power law

$$I = I_o \nu^{\alpha}$$

where α is referred to as the spectral index and varies from -1 to -2.[7] Spectral studies to date have poor resolution taking only four or five points from 100 to 10,000 MHz with more thorough studies taking 10 points. Similar to the frequency dependence of the pulse separation, there seems to be a break frequency for the spectra of pulsars above which the spectral index changes to a more negative value causing the

spectrum to fall off faster. Although this is not observed in all pulsars this may be due to the limitations of the measurement range. It has been noted that the spectral index is not the same for different pulse peaks in a complex pulse profile. They can vary by as much as a factor of two for the precursor pulse of the Crab Pulsar for the high frequency end of its spectrum. Most spectra show a low frequency cutoff frequency at about 100 MHz. This frequency is the low end of most spectral measurements and pulsars which do not display this cutoff may have one at a lower frequency.

Another important characteristic displayed by pulsars is a high degree of polarization. The polarization observed is both linear and circular with the linear polarization dominating and sometimes reaching 100% of the pulse intensity. The circular polarization is usually 20% or less. The polarization is really a feature of the individual pulses and integrating has a tendency of reducing the percentage of polarization. The degree of polarization appears to be a function of frequency, decreasing in general with increasing frequency. The manner in which it falls off varies greatly from pulsar to pulsar. In some cases it remains fairly constant throughout the observed spectrum. In other cases it remains constant up until a break frequency after which it falls as some power law. The polarization angle sweeps through a range of positions up to about 150^{o} across the pulse profile. Type S pulsars usually display the least amount of angle change and type C pulsars display the greatest change in position angle.[8] The change in angle is the greatest in the center of the pulse profile and least in the wings.

Single Pulse Characteristics

Since pulsar signals are such low intensity sources, it is more difficult to measure their characteristics than for integrated pulse profiles. For this reason the data for single pulses is not as extensive as that for the integrated pulses. Even so measurements taken for a number of pulsars with low dispersions have identified a number of class characteristics of the individual pulses or subpulses. Due to their nature the subpulses appear to give information about the emission mechanism and the radiative transfer processes in the magnetosphere of the pulsar.

The first notable feature is that the subpulse has a different shape than the integrated pulse profile, being roughly Gaussian. The subpulses usually have widths of between 1 and 4 percent of the pulse period and occur at various longitudes in the integrated pulse profile.[9] The width of the subpulse in relation to the integrated pulse seems to be a function of pulse period with the longer period pulsars having subpulses much narrower than the integrated pulse profile. The width is roughly a function of the square root of the period. The width of the subpulses does not seem to depend on frequency or the location of the pulse in the integrated pulse profile. The spectrum of the subpulses in PSR 1919 +21 is similar to the spectrum for its integrated pulse and this is probably true of most pulsars.[10]

The intensity of individual pulses varies greatly from pulse to pulse. Some pulses are missed completely in a process referred to as nulling. Most of the observed pulsars seem to exhibit this nulling feature in their pulse train. The nulling may take place anywhere from 10 to 75 percent of the time.[11] Spectral studies have been made to deter-

mine whether there is any regularity to the nulling pattern. In most pulsars especially the short period group, P $\leq$ .75 sec., the distribution of the nulling patterns seems to be random. For other pulsars, however, there are sharp peaks in the frequency of occurrence distribution of the nulling.[12] The frequency of the nulling varies from one null every 50 cycles to the Nyquist frequency of half the sampling rate of the pulsar's frequency. Type C pulsars occasionally have their subpulses vary in such a manner that some of the components vary regularly while others vary randomly. When this happens very often the regularly varying components will occur in pairs. In PSR 1237 + 25 the two outer components vary at the same rate while the inner components have random variations.[13]

The amount of variation or the modulation of the pulses is a function of the frequency with the fluctuations at the lower frequencies being more pronounced. The fluctuations also seem to vary with location within the integrated pulse profile, with the subpulses of some of the components having a greater range of modulation than those of another. Multiple peak profiles often have pairs of peaks which vary in the same manner while others vary in a different way. In type S pulsars the subpulses at different locations in the integrated pulse profile often have different degrees of modulation. It is important to note that the nulling effect may be characterized by its random and its periodic nature.

Drifting subpulses are one of the most interesting aspects of the pulsar radiation.[14] This is a phenomenon where the subpulse train of certain pulsars is such that each subpulse is displaced by a certain amount in longitude, usually from the trailing edge to the leading edge of the pulse profile. When the pulse reaches the leading edge it reappears at the trailing edge and repeats the motion. Sometimes more

than one subpulse will participate in the action and the subpulse will drift together across the integrated profile. For pulsars PSR 0031 - 07 and PSR 0809 + 74 the spacing of the pulses varies with the frequency in the same manner as the integrated pulse.[15] Some pulsars show a less regular drift. Instead of drifting across the entire profile the subpulse will only drift slightly about some mean position. This drift is usually detected by the use of a cross-correlation signal processing technique. The successive pulses are cross-correlated and any variation of the correlation peak from a time different from the pulse period is noted. As a rule type SD pulsars show these slight drifts of peaks from the trailing edge to the leading edge of the pulse profile and have small rates of change of pulsar spin, $\dot{P}$. The type CD pulsars have their subpulses drift from the leading edge to the trailing edge of the pulse profile and the rate of change of the pulsar spin $\dot{P}$ is large. The drift rate of the subpulses is usually not a constant throughout the pulse profile and the greatest drift occurs at the edges.

The next refinement in time resolution of the subpulses gives them structure known as micropulses.[16] These may only be seen for pulsars with very low dispersions since otherwise the de-chirping signal processing technique fails. At this resolution we can see structure down to the microsecond scale, which is about the limit of resolution for the technique. The width of the micropulses seems to be independent of frequency. The micropulses also seem to show some periodic structure.[17]

As noted previously, the integrated pulse shows a wide range of polarizations varying from 20 to 100 per cent. Since the integrated pulse is composed of a period average of the subpulses, the degree of polarization may be due to three causes. First the subpulses themselves

may or may not have a great degree of polarization. Second the subpulses may be polarized but successive subpulses may have orthogonal polarizations. Third the subpulses may be polarized with random angles from pulse to pulse. All three of these characteristics are observed in pulsar radiation.

Most subpulses have a high degree of linear polarization with some circular polarization.[18] The position angle of the polarization varies throughout the integrated pulse profile usually in a smooth manner by 30 percent or less. The degree of polarization may differ from component to component during a pulse anywhere from 20 to 100 percent. In some pulsars the position angle is very stable with position in the integrated pulse profile but the degree of polarization will vary greatly from pulse to pulse. Both the degree of polarization and the position angle seem to be more stable at the lower frequencies.

The polarization of the subpulses is probably a more significant feature of the pulsar radiation than the polarization of integrated pulse since one determines the other. Likewise the polarization of the micropulses is of greater importance than the polarization of the subpulses. These, however, are very difficult to measure and only those pulsars with very low dispersion may be analyzed. The data are not very extensive but the micropulses seem to have a high degree of polarization as one would expect. There seems to be a variability of the polarization angle between adjacent micropulses which tends to reduce the polarization of the subpulse. In some cases the polarization angle will make abrupt changes of up to 180^{o} between two micropulses.[19]

Summary

As may be seen from the preceding discussion of pulsar observations the radiation from pulsars exhibit many strong characteristics. Without a structure to base an interpretation, they seem very diverse and confusing. This confusion is due to the great variability of the radiation characteristics from pulse to pulse. In this work we assume that the variation has two sources. First is the variability in the conditions of the plasma in the region of emission. Here, the production of the radiation and the transfer of the radiation are highly dependent on the distribution of the plasma in this region. Since the plasma is thought to be flowing at a great speed, turbulence effects are possible which could lead to the resultant variability of the emission. The second cause of the variability may be thought to be due to changes in the orientation of the magnetic field of the star with respect to the observer. Since the beam of radiation is tied to the orientation of the magnetic field, any changes in orientation due to rotation of the star or the generation of secondary magnetic fields by the current flow from the surface would produce changes in the observed radiation. With these assumptions we may first study a steady state problem and then add these aspects of the variability to produce the observed radiation. This is the plan of attack used in this study.

FOOTNOTES

[1]F. R. Smith, Pulsars (Cambridge University Press, Cambridge, 1977) Chapter 2.

[2]A. E. Vaughan and M. I. Large, Proc. Astron. Soc. Australia 1, 220 (1969).

[3]V. V. Zheleznyakov and V. L. Ginzburg, Ann. Rev. Astron. Astrophys. 13, 511 (1975).

[4]G. P. Huguenin, J. H. Taylor and T. H. Troland, Astrophys. Jour. 162, 727 (1970).

[5]W. Sieber, R. Reinecke and R. Wielebinski, Astron. Astrophys. 38, 169 (1975).

[6]Ibid.

[7]W. Sieber, Astron. Astrophys. 28, 237 (1973).

[8]R. N. Manchester, Astrophys. Jour. Supp. 23, 283 (1971).

[9]J. H. Taylor, R. N. Manchester and G. R. Huguenin, Astrophys. Jour. 195, 513 (1975).

[10]B. J. Robinson, B. F. C. Cooper, F. Gardner and R. Wielebinski, Nature 218, 1143 (1968).

[11]D. C. Backer, Astrophys. Jour. 182, 245 (1973).

[12]J. H. Taylor and G. R. Huguenin, Astrophys. Jour. 167, 273 (1971).

[13]D. C. Backer, op. cit.

[14]F. D. Drake and H. D. Craft, Nature 220, 231 (1968).

[15]J. H. Taylor, R. N. Manchester and G. P. Huguenin, Astrophys. Jour. 195, 513 (1975).

[16]H. D. Craft, J. M. Comella and F. D. Drake, Nature 218, 1128 (1968).

[17]T. H. Hankins, Astrophys. Jour. 169, 487 (1971).

[18]R. N. Manchester, J. H. Taylor and G. P. Huguenin, Astrophys. Jour. 196, 83 (1975).

[19]J. M. Cordes, Astrophys. Jour. 195, 193 (1975).

CHAPTER III

RADIATION MECHANISM THEORIES AND A CALCULATION FOR THE SPECTRUM OF A LINEARLY ACCELERATED CHARGE

At the present time there are about six viable theories to explain the source of the radiation from pulsars.[1-6] That this many theories exist is due mainly to the inability of any one of them to give much more than a qualitative argument for its existence. The manner in which the theories are developed consists in first postulating a condition within the magnetosphere and showing that it is reasonable. This condition is then shown to give rise to radiation, and the spectrum is compared to observations. The problem with these theories is that the equations involved are beyond present means of solution. This means that approximations must be made and this usually has a tendency of obscuring the results. The results then tend to be accurate to an order of magnitude and they establish more the possibility than the probability.

The purpose of this section of the study is to calculate the spectrum of a linearly accelerated charge under the conditions thought to exist in the pulsar's magnetosphere. Although this would seem to be one of the simpler causes, it has previously been regarded as beyond the reach of mathematical techniques available. This view has changed, however, with the introduction of fast Fourier transform techniques. Admittedly, even this calculation is dependent on simplifications which may

modify the results in some manner. The calculation is, however, a step in the right direction.

For this part of the study we will first look at some of the better accepted radiation mechanisms. We will then look at the development of the linear acceleration radiation mechanism. A calculation of the radiation spectrum will be presented using parameters assumed to exist in the magnetosphere of a neutron star. This spectrum will then be compared to observations.

Radiation Mechanisms

The radiation mechanisms may be divided into three categories: those which originate near the surface of the star, those that have their origin near the light cylinder and those sources outside the co-rotating zone. At the present time those theories which postulate sources near the surface of the star in the region of the open field lines seem to have the largest following.

In the region outside the light cylinder we would enter the radiation zone ($r < \lambda$) for the low frequency radiation of the pulsar. This low frequency radiation is caused by the star's rotating dipole field. This field is extremely intense and, since its frequency is much below the cutoff frequency for the surroudning plasma, its radiation pressure is thought to clear a cavity about the star. The boundary is determined by the point where the gas pressure of the surrounding interstellar matter is equal to the radiation pressure. Since the field strength of the radiation varies with the rotation of the star, the boundary of the cavity pulsates at the frequency of the pulsar. It is the pulsation of the boundary of the cavity which is thought to produce the radiation.

Since the charges have been accelerated to relativistic speeds by the pulsars electric field, the acceleration of these charges in the pulsating envelope will produce radiation. This theory has a number of problems. The most basic of which is the assumed density of the plasma at the boundary. Calculations by Rees and Gunn[7] show that the density of the plasma at the boundary would be much less than that proposed by Lerche.[8] Also the large distance from the star would mean that the magnetic field would have the configuration of a dipole. This would make asymmetries in the location of the interpulse very hard to explain. The great stability of the pulse profile would require a similar stability of the diffuse plasma in this region which is hard to realize physically. Further calculations show that radiation produced in this manner would produce a continuous spectrum which is not observed in the case of the Vela and Crab pulsars.[9]

The theories predicting the source to be located near the light cylinder are attractive because they make available the relativistic beaming process to explain the narrow pulse of radiation. As is described in a number of texts, when an isotropic radiation source moves with a relativistic velocity the radiation becomes anisotropic in the direction of the velocity vector.[10] The angular width of the radiation is a function of the relativistic factor $\gamma = (1 - v^2/c^2)^{-\frac{1}{2}}$. If the relativistic factor is large enough, it can significantly enhance the radiation intensity in this manner. For pulsars with complex pulse profiles the radiation could originate in two or more regions which would produce different peaks. In this model the radiating region corotates with the star. Each time the velocity vector of the radiating region points at the observer he will see a pulse. This beaming effect is

independent of the manner in which the radiation is produced. Zheleznyakov has shown that if the spectrum of the radiation mechanism is written as a power series, the form will be preserved by this beaming mechanism.[10] This is shown by the expressions for the intensity $S(\nu)$

$$S(\nu) = E\nu^{\alpha} \qquad \text{Moving Frame}$$

$$S(\nu) = E\gamma^{\alpha-3}\,(1 - \cos\theta \sin i)^{\alpha-3}\nu^{\alpha} \qquad \text{Observer's Frame}$$

where α is the spectral index, i is the angle between the rotational axis and the observer's line of sight, θ is the angle between the velocity vector of the rotating source and the observer's line of sight and γ is the relativistic factor. The two emission mechanisms which have been proposed to explain the radiation are cyclotron radiation by electron bunches and a maser mechanism which uses the energy levels of the electron revolving about the magnetic fields.[12,13] Both of these mechanisms produce highly polarized radiation and it has been shown that the radiation observed from these sources would change its angle of polarization in a manner similar to that observed. The light cylinder models are also beset with a number of problems. Foremost of these is the calculation which sets severe restrictions on the distance out to which the magnetosphere may rotate. It has been shown that the magnetosphere will only corotate out to a point that its velocity is less than the Alfven velocity, the velocity of plasma waves.[14] This drastically reduces the relativistic factor with a v/c ratio of .71 as a maximum. If this is the case the beaming mechanism will no longer be available to the theory. The predicted dependence of the beam width with the spectral index has not been observed either. Another problem deals with the lack of depend-

ence of the spectral characteristics with pulse period. Since the proposed radiation mechanism is dependent on magnetic field strength and the magnetic field is dependent on the distance from the star, the characteristics of the pulsar radiation should be a function of the period, the extent of the magnetosphere and the distance to the light cylinder being a function of this period. Finally, the observed stability of the pulse profile is hard to justify with the radiation source near the light cylinder. The magnetic field at this point is much weaker and the magnetosphere would be expected to be quite turbulent in this region.

The third region of interest for producing radiation lies above the surface of the star in the area where the open field lines originate. Open field lines are the magnetic field lines which extend past the light cylinder and originate at the magnetic poles. This region has been proposed for a number of reasons. First is the great stability of the region due to the strength of the magnetic field there. Next is the large electric field which is expected to exist there and which should be capable of accelerating charges to relativistic speeds. Any multipole moments of the magnetic field would be evident close to the surface of the star and could manifest themselves as pulse structure. Explaining the charge separation in this region is a direct consequence of Julian's and Goldreich's magnetosphere model.[15]

The various radiation mechanisms for this region depend on the charges being accelerated to relativistic speeds from the surface of the star while following the open field lines. Three devices have been proposed for producing the radiation along with some variations. First is curvature radiation. In which case the radiation is produced by the acceleration given to the electrons as they travel along the curved path

of the magnetic dipole field lines. For this theory to be successful, a mechanism to produce coherence in the radiation must be introduced. This is needed to explain the intensity of the observed radiation. The usual method employed is to postulate some mechanism which will bunch the radiation into regions with thicknesses less than a wavelength of the radiation observed. In this case the charges in the bunch would emit radiation approximately in phase so that their fields, not their intensities, would add. The intensity of the radiation would then go as N^2 (not N) where N is the density of the plasma.

The variations in the curvature radiation theory are due to different proposals for the manner in which the charge bunches are produced. Sturrock proposed that electron-positron pairs would be produced in the intense radiation fields near the surface of the star. These pairs would separate in the strong electric field and produce an opposing field of their own. This field would reach a point where it would cut off the flow from the surface until the electron-positron pairs separation produced a field strong enough to produce secondary electron-positron pairs. This process would produce a fluctuating charge flow which could produce bunching of the charges.[16] Goldreich and Keeley proposed that a mechanism based on the instability of charges moving in a curved path could produce bunching.[17] Rudermann and Sutherland proposed that a two-stream instability could be capable of producing density waves in the plasma. Using a mechanism similar to Sturrock's for producing electron-positron pairs, they proposed that the escaping positrons would produce these waves in the slower moving plasma surrounding the star.[18] This work will investigate the creation of bunches due to the growth of instabilities in a supersonic plasma. The basic argument against bunching mechanisms,

however, is that the bunches will dissipate in a very short time, typically 10^{-8} second if the plasma has even a minimal velocity distribution.

Another radiation mechanism which has been proposed is magneto-bremstrahlung radiation.[19] The magnetic field about the star is strong enough so that the orbits which the electrons make about the field direction will have radii of the order of the deBroglie wavelength of the electrons. This means that the electron orbits should be treated quantum mechanically. The energy levels of the electrons in these orbit orbits are quantized in what are familiar as Landau levels. Electrons which are emitted from the surface of the star at an angle to the magnetic field will fall in one of these levels and transitions between levels will produce radiation. In this model the electrons interact with ions in the plasma (this model is not charge separated) and a reaction

$$e^{-}(n) + (Z,A) \rightarrow e^{-}(n') + (Z,A) + \gamma$$

will take place. This reaction is capable of producing a continuum spectrum for the radiation rather than the discrete lines expected from the quantized levels. To produce the desired energy flux a maser mechanism is proposed which uses an inverted population of the electrons in the Landau levels as a source of the stimulated radiation.

A third radiation mechanism, and the one which we will be dealing with in this work, is due to the linear acceleration of charges from the surface of the star. This mechanism was first proposed by Kaplan and Eidmann[20] and later discussed by Cocke[21] and Melrose.[22] Whereas Kaplan's and Eidmann's paper presented linear acceleration radiation for comparison purposes with curvature radiation, Cocke and Melrose made calcula-

tions to give values to the upper and lower bounds of the frequency and signal strength. Both Cocke and Melrose proposed a maser mechanism to explain the observed intensity of the radiation. Both treatments suffer from a lack of an exact treatment of the spectrum of the radiation. Also the exact mechanism by which the electrons change their energy levels under the stimulated emission is not clear. The next section will offer a solution for the approximate spectrum.

The model which we use makes a number of assumptions to facilitate the calculation. We treat a situation in which electrons leave the surface of the star under the influence of an electric field which may have values up to 10^{12} V/m but which is probably smaller than that. The magnetic field is treated as having very little curvature so that the trajectory of the electron will be linear. The electric field is treated as being constant although this is most probably not the case. Since the field strength is of the order of 10^{12} V/m the motion of the electron will be relativistic. In the next section we derive the kinematic expressions needed to calculate the energy spectrum.

Equation of Motion for Linearly Accelerated Charge

The relativistic treatment of a charge moving under the influence of an electric field has been treated a number of times in the literature.[23,24] We wish to relate the kinematic expressions for position, velocity and acceleration inthe observer's frame to the acceleration of a particle in its moving reference frame. We choose the charge's frame as that in which the charge is momentarily at rest. The charge's frame is moving parallel to both the accelerating electric field and the

magnetic field. The Lorentz transformation of these fields to the particle's frame leaves them unchanged. In that case we get an acceleration of the charge in this frame of

$$\vec{a}^{+} = \frac{\vec{F}}{m} = \frac{e\,\vec{E}}{m} \tag{1}$$

where e and m are the charge and mass on the electron. The theory of relativity may be formulated in a manner which introduces four component vectors representing position, displacement, velocity and acceleration in space-time. If transformations are made between inertial reference frames in such a manner so as to preserve the speed of light, we find that the kinematic quantities have scalar products which are invariant. Thus for a change in the position vector $x^i = (ct, x, y, z)$ the distance given by (our metric here is $g^i_i = (1, -1, -1, -1)$)

$$ds = (c^2dt^2 - dx^2 - dy^2 - dz^2)^{\frac{1}{2}}, \tag{2}$$

must be the same in all inertial systems. The 4-vector velocity is formed by taking the derivative of the position 4-vector with respect to the change in position of the particle in 4-space, i.e. ds. Noting that

$$ds = c\,dt\sqrt{1 - \frac{dx^2}{dt} - \frac{dy^2}{dt} - \frac{dz^2}{dt}} = c\,dt\sqrt{1 - \frac{v^2}{c^2}}, \tag{3}$$

we get the 4-velocity

$$u^i = \frac{dx^i}{ds} = \left(\frac{1}{\sqrt{1 - (v/c)^2}}, \frac{\vec{v}}{c\sqrt{1 - (v/c)^2}}\right), \tag{4}$$

which has the magnitude

$$u^i u_i = 1, \tag{5}$$

for all inertial reference frames. Likewise we may find the 4-acceleration defined as

$$a^i = \frac{du^i}{ds} = \left(\frac{\vec{v} \cdot \frac{d\vec{v}}{dt}}{c^3(1 - v^2/c^2)^2}, \frac{\frac{d\vec{v}}{dt} - \frac{v^2}{c^2}\frac{d\vec{v}}{dt} + \frac{\vec{v}}{c^2}\vec{v} \cdot \frac{d\vec{v}}{dt}}{c^2(1 - v^2/c^2)^2} \right), \tag{6}$$

where the magnitude in 4-space is

$$a^i a_i = -\frac{a^{+2}}{c^4}. \tag{7}$$

Here a^+ is the acceleration in the reference frame where the particles instantaneous velocity is zero. We use the invariance of the acceleration 4-vector to relate acceleration in the particles instantaneous inertial frame to the observer's frame. For our problem the velocity and acceleration are parallel so the acceleration is given by

$$a^i = \left(\frac{\vec{v} \cdot \frac{d\vec{v}}{dt}}{c^3(1 - v^2/c^2)^2}, \frac{\frac{d\vec{v}}{dt}}{c^2(1 - v^2/c^2)^2} \right). \tag{8}$$

The scalar product $a^i a_i$ gives a relation for the acceleration in the observer's frame to the acceleration in the charges instantaneous rest frame

$$a^+ = \frac{\frac{dv}{dt}}{[1 - v^2/c^2]^{3/2}}. \tag{9}$$

Noting that the expression on the right is an exact differential we have by integrating

$$\frac{v}{\left[1 - \frac{v^2}{c^2}\right]^{1/2}} = a^+ t, \tag{10}$$

where we assume the initial conditions t = 0, v = 0. Solving for velocity

$$v = \frac{dx}{dt} = \frac{a^+ t}{\left[1 + \left(\frac{a^+ t}{c}\right)^2\right]^{1/2}} \tag{11}$$

We then substitute this expression in the expression for the acceleration of the particles rest frame, eq. 9, to give us an expression relating the acceleration of the particle in its rest frame to the observed acceleration.

$$a = \frac{dv}{dt} = \frac{a^+}{\left[1 + \left(\frac{a^+ t}{c}\right)^2\right]^{3/2}} \tag{12}$$

By integrating the expression for the relative velocity of the two frames we may get the position of the particle in the observer's frame.

$$x(t) = \frac{c^2}{a^+}\sqrt{1 + \left(\frac{a^+ t}{c}\right)^2} - \frac{c^2}{a^+}, \tag{13}$$

where we have the initial conditions x = 0 at t = 0. With these kinematic expressions in the observer's frame we can calculate the spectrum using the Lienard-Wiechert theory.

Retarded Radiation Fields and Their Spectral Analysis.

Finding the spectrum of the radiation from an accelerated charge consists of first finding the expression for the radiated or acceleration field. Next, finding the energy of this field and then taking the Fourier transform of the energy. Care must be taken to account for the finite speed of propagation of this radiation. The expression for the radiated electric field due to accelerated charges is given by the Lienard-Weichert theory as[25]

$$\vec{E}(x,t) = \frac{e}{c} \left\{ \frac{\hat{n} \times [\hat{n}-\vec{\beta}] \times \dot{\vec{\beta}}}{(1 - \hat{n}\cdot\vec{\beta})^3 R} \right\}_{RET} \tag{14}$$

where $\hat{n}$ is the unit vector in the direction of the observer, $\vec{\beta}$ and $\dot{\vec{\beta}}$ are the velocity and acceleration divided by the speed of light, R is the distance to the observer and RET means that the time at which $\vec{\beta}$ and $\dot{\vec{\beta}}$ are evaluated is equal to the time of observation of the radiation minus the time of propagation.

The angular distribution of the radiated power is given by

$$\frac{dP}{d\Omega} = \frac{c}{4\pi} [R\, E(x,t)]^2 , \tag{15}$$

where $d\Omega = dA\, R^{-2}$ = solid angle into which the power is radiated. The differential energy is then

$$\frac{d\varepsilon}{d\Omega} = \frac{c}{4\pi} \int_{-\infty}^{\infty} \left| R\, E(x,t) \right|^2 dt . \tag{16}$$

If the Fourier transform of the field is given by

$$E(x,\omega) = \frac{1}{\sqrt{2\pi}} \int_{-\infty}^{\infty} dt\, E(x,t) e^{i\omega t} , \tag{17}$$

then Parseval's theorem gives us

$$\frac{d\varepsilon}{d\Omega} = \frac{c}{4\pi} \int_{-\infty}^{\infty} \left| R\, E(x,\omega) \right|^2 d\omega . \tag{18}$$

This means that the integrand is the energy per unit angle per unit frequency, the quantity of interest. Substituting the expression for the retarded electric field, eq. 14 we get

$$\frac{d^2\varepsilon}{d\Omega d\omega} = \frac{e^2}{8\pi^2 c} \left| \int_{-\infty}^{\infty} \left[\frac{\hat{n} \times \{(\hat{n}-\vec{\beta}) \times \dot{\vec{\beta}}\}}{(1 - \vec{\beta}\cdot\hat{n})^3} \right]_{RET} e^{i\omega t}\, dt \right|^2 . \tag{19}$$

To evaluate the integral we must convert the observer's time to the retarded time. To do this we suppose that the observer is very far away from the region in which the radiation is being emitted. In this case the angle of observation is constant in time and we may make the approximation

$$t = t' + \frac{\vec{R}'(t')}{c} \cong t' + \frac{\vec{R} - \vec{r}(t')\cdot\hat{n}}{c} . \tag{20}$$

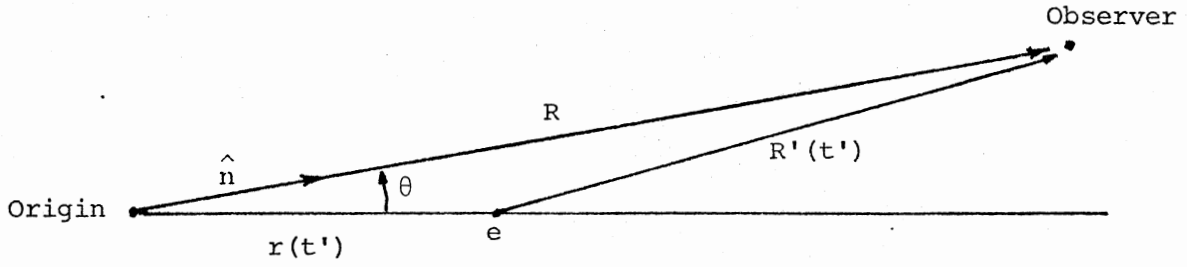

Here $\hat{n}$ is the unit vector to the observer, r(t') is the position of the charge R is the distance from the origin to the observer, R(t') is the distance from the charge to the observer, t is the observer's time and t' is the charge's time. The integral in terms of the charge's time then becomes

$$\frac{d^2I}{d\Omega d\omega} = \frac{e^2}{4\pi^2 c}\left|\int_{-\infty}^{\infty} dt' \frac{\hat{n}x\{(\hat{n}-\vec{\beta})x\dot{\vec{\beta}}\}}{(1-\vec{\beta}\cdot\hat{n})^2} e^{i\omega(t' + \frac{\vec{R}-\hat{n}\cdot\vec{r}(t')}{c})}\right|^2 \qquad (21)$$

where $\vec{r}(t')$, $\vec{\beta}(t')$ and $\dot{\vec{\beta}}(t')$ are the previously derived kinematic expressions, eqns. 11, 12, 13.

For the geometry of this problem we have $\vec{r}(t')$, $\vec{\beta}(t')$ and $\dot{\vec{\beta}}(t')$ all parallel. In this case the expression in the numerator becomes, using the identity for the triple cross-product and the fact that $\vec{\beta}(t')x\dot{\vec{\beta}}(t') = 0$,

$$\vec{n}x\{\hat{n}-\vec{\beta})x\dot{\vec{\beta}}\} = \hat{n}x(\hat{n}x\dot{\vec{\beta}}) - \hat{n}x(\vec{\beta}x\dot{\vec{\beta}}) = \dot{\beta}(\hat{n}\cos\theta - \dot{\vec{\beta}}) \qquad (22)$$

Note that this is a vector in the plane of $\hat{n}$ and $\dot{\vec{\beta}}$. Since for large distances the angle of propagation is nearly constant we may remove the vector factor from the integral and evaluate its absolute value giving

$$|\hat{n}\cos\theta - \dot{\vec{\beta}}|^2 = \sin^2\theta \qquad (23)$$

and the integral where we have also removed the phase factor EXP($i\omega\frac{R}{c}$)

$$\frac{d^2I}{d\Omega d\omega} = \frac{e^2}{4\pi^2 c}\sin^2\theta\left|\int_{-\infty}^{\infty} \cdot\, dt \frac{\dot{\beta}\, e^{i\omega(t - \frac{n\cdot r(t)}{c})}}{(1 - \beta\cos\theta)^2}\right|^2 \qquad (24)$$

In order to find the spectrum we must evaluate this integral. This problem is intractable using normal methods. However, with a change in variables it lends itself to solution by numerical methods. The development of a fast Fourier transform algorithm allows us to evaluate this integral in a rather short period of time at a number of different angles of observation with a minicomputer. In order to do this calculation, however, we must change the argument in the exponential to the form $i\Omega T$. Substituting the kinematic expression for position in the exponential we have

$$\mathrm{EXP}\left\{ i\omega\left(t - \frac{\cos\theta}{c}\left[\frac{c^2}{a^+}\sqrt{1 + \left(\frac{a^+ t}{c}\right)^2} - \frac{c^2}{a^+}\right]\right)\right\} . \tag{25}$$

We first separate out the phase factor $\mathrm{EXP}(i\omega \frac{c}{a^+}\cos\theta)$ and then make the substitutions

$$\Omega = \frac{c\omega}{a^+} , \quad T' = \frac{at}{c} \text{ and } T = T' - \cos\theta\sqrt{1 + T'^2} . \tag{26}$$

This will give us the exponential with an argument of $i\Omega T$.

The inverse transformation is

$$\frac{at}{c} = T' = \frac{T \pm \cos\theta\sqrt{T^2 + \sin^2\theta}}{\sin^2\theta} . \tag{27}$$

This gives us two roots to choose from. In order to choose the correct one we look at the transformation's behavior about the angle $\theta = 0$. From the formula for the change in variables we see that the inverse

function should be

$$T = T' - \sqrt{1 + T'^2} \quad , \quad T' = \frac{T^2 - 1}{2T} \quad . \tag{28}$$

Taking the limit of the inverse transformation with the positive root we get a discontinuity at $\theta = 0$ but the limit of the transformation with the negative root gives the correct form.

Using this inverse transformation we form the differential dT'

$$\frac{a}{c}\, dt = dT' = \frac{1 - \dfrac{T \cos\theta}{\sqrt{T^2 + \sin^2\theta}}}{\sin^2\theta}\, dT \quad . \tag{29}$$

The expressions for the kinematic quantities in the transformed variable are

$$\beta = \frac{T - \cos\theta \sqrt{T^2 + \sin^2\theta}}{\sqrt{T^2 + \sin^2\theta} - T \cos\theta} \quad , \tag{30}$$

$$\dot{\beta} = \frac{\dfrac{a^+}{c} \sin^6\theta}{\left[\sqrt{T^2 + \sin^2\theta} - T \cos\theta\right]^3} \quad . \tag{31}$$

Substituting these in the integral we have

$$\frac{d^2 I}{d\Omega d\omega} = \frac{e^2 \sin^2\theta}{4\pi^2 c} \left| \int_{-\cos\theta}^{\infty} \frac{dT \sin^4\theta\, e^{i\Omega T}\, e^{i\Omega \cos\theta}}{\sqrt{T^2+\sin^2\theta}\, \left(\sqrt{T^2+\sin^2\theta}\, (1+\cos^2\theta) - 2T\cos\theta\right)^2} \right|^2 , \tag{32}$$

where the limits of integration reflect the fact that $\dot{\beta} = 0$ for all $t<0$. Letting $u = T + \cos\theta$, $du = dT$ and $T = u - \cos\theta$. Which gives the integral

$$\frac{d^2I}{d\Omega d\omega} = \frac{e^2\sin^2\theta}{4\pi^2 c}\left|\int_0^{\infty} \frac{du\ \sin^4\theta\ e^{i\Omega u}}{\sqrt{u^2-2u\cos\theta+1}\ \left[\sqrt{u^2-24\cos\theta+1}\ (1+\cos^2\theta)-2u\cos\theta+2\cos^2\theta\right]^2}\right|^2. \tag{33}$$

The integral is now in a form which may be transformed using the FFT algorithm. The program is given in the Appendix with an explanation of its use. The program was run for every 5 degrees of angle and the results are given in the next section and compared with the experimental data.

Results

From the program we were able to bet both an angular and a frequency distribution of the radiated energy. The most obvious aspect of the data is that the shapes of the distributions are invariant to the accelerating field, which enters the problem only as a scaling factor on the frequency axis. The log-log plot, Figure 1, of the energy spectrum shows that the energy falls off very slowly for low frequencies and then drops off as an increasing power of frequency until it falls off as a power of -2.5. There is no low frequency cutoff.

The angular distribution, Figure 2, shows that the radiation pattern depends on the frequency in two ways. First, the angular width of the beam is an inverse function of the frequency being extremely broad for the low frequencies and very narrow for higher frequencies. Second, the direction of the maximum propagation is also a function of frequency.

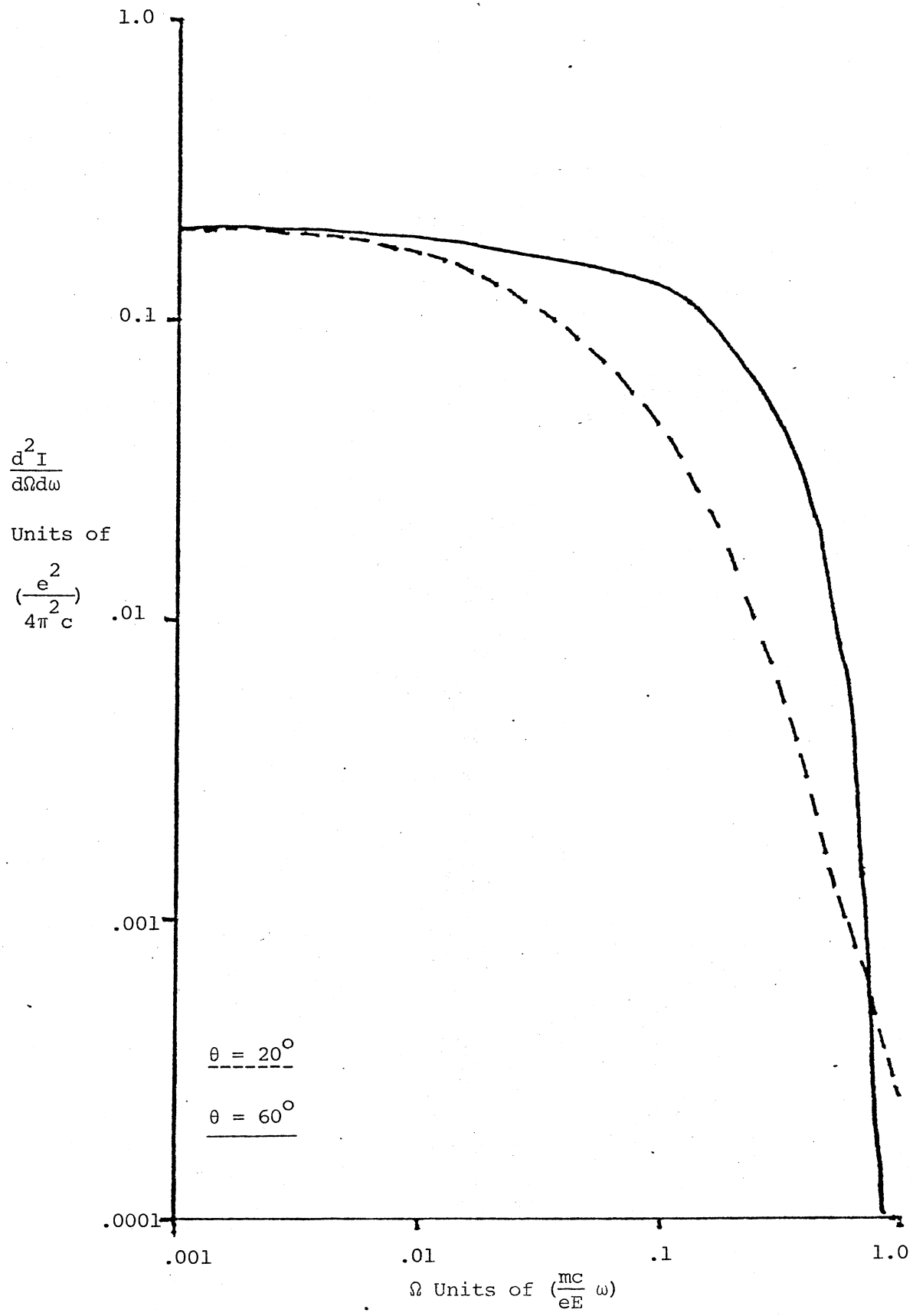

Figure 1. Log-Log Plot of Differential Intensity Vs. Frequency

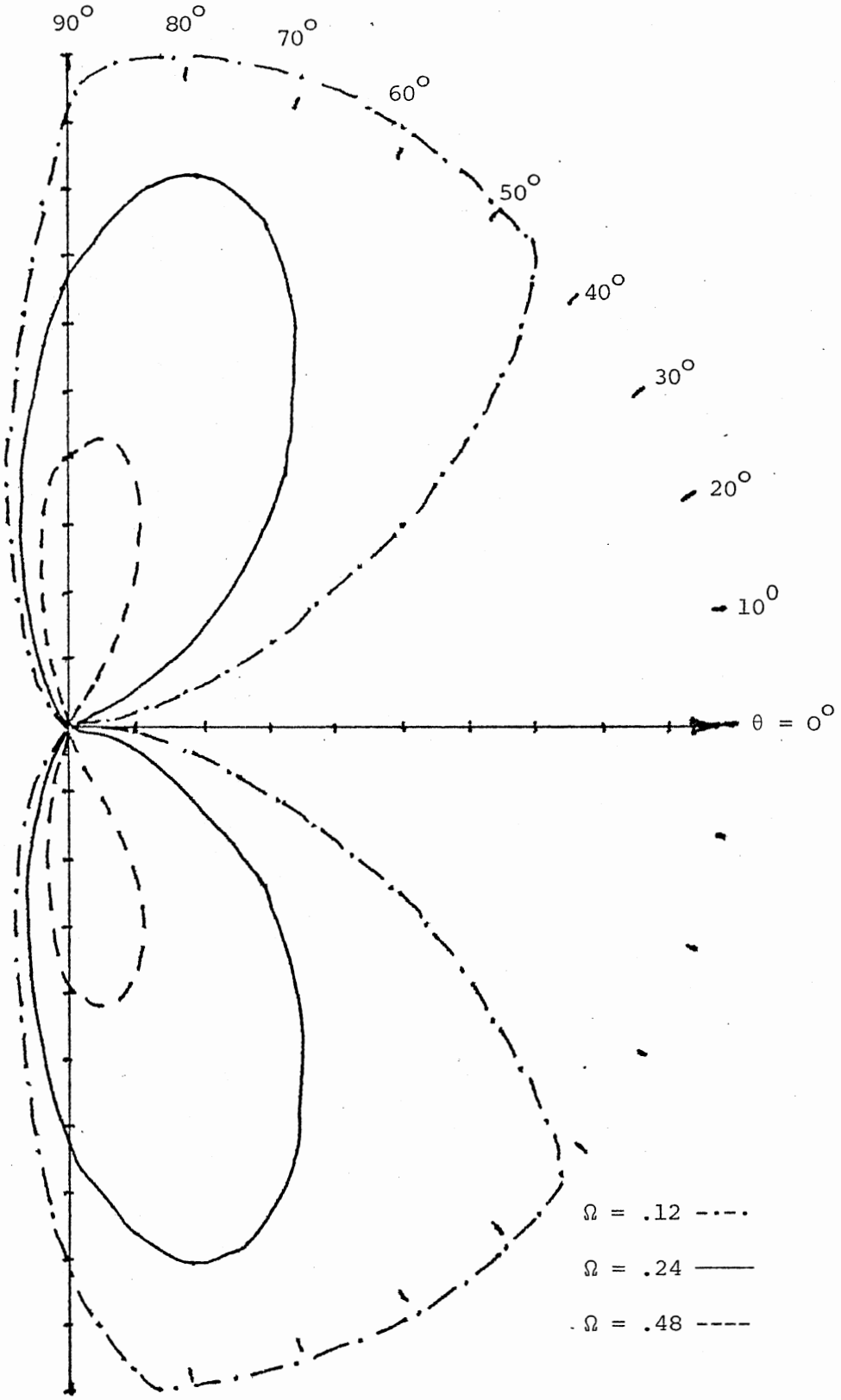

Figure 2. Radiation Pattern for Linearly Accelerated Charge

As may be seen from the polar plot, the angle between the charges velocity vector and the radiation's wavevector is an increasing function of frequency. It ranges from 60^{o} for low frequencies to 90^{o} for high frequencies. There is negligible propagation in the forward direction as would be expected from the severe restriction imposed by the $\sin^{10}\theta$ factor in the expression.

The first impression given by the results is that something is wrong. The literature on the angular distribution of radiation by a linearly accelerating charge indicates that for large relativistic factors β, the radiation pattern will be angled in the forward direction from the Larmor pattern which has a $\sin^{2}\theta$ dependence.[26] This is usually explained by looking at the integrand for the expression giving the energy radiated per unit area

$$\frac{\dot{\beta}^{2} \sin^{2}\theta}{[1 - \beta \cos\theta]^{5}} .$$

When the relativistic factor β approaches 1, the denominator of the expression becomes very small for small values of θ. The expression then becomes very large and this argument is used to show that the radiation is beamed in the forward direction. In our case, however, the acceleration and velocity factors are related with $\dot{\beta}$ going to zero faster than β goes to one. This means that the expression will go to zero for high velocities rather than become large. It is noted that nearly all the radiation takes place in the forward direction approaching 90^{o} for the higher frequencies. For high frequencies the angular distribution of the radiation approaches the Larmor from which goes as $\sin^{2}\theta$. The explanation for this is found by looking at the shape of the radiated

pulse in time. We see that the pulse strength increases in a very short time to a maximum and then falls off at a much slower rate. At the beginning of the particles trajectory the velocity is non-relativistic and the acceleration is its maximum. This rapid increase in field strength would be expected to give rise to a broad band of radiation and, since the particle's speed is relatively low, the angular distribution would be close to the Larmor form. After the particle reaches relativistic speeds the acceleration, and therefore the field intensity, falls off more gradually. It would be expected that this change in field strength would give rise to low frequency radiation but now the particle is relativistic so we would expect a more forward type radiation pattern. This explanation would seem to account for the broad pattern for the low frequency signals and the Larmor-like pattern for the higher frequencies. This effect, however, is not what is observed in pulsar radiation. The width of the pulse seems to be a function of frequency with the higher frequency pulses being narrower than the lower frequency pulses. This is also shown by looking at the separation of the components of two pulse profiles. The separation of the pulses is an inverse power function of the frequency of observation. The separation index of a typical double peaked pulse is about -.25 where

$$\Delta\phi = \nu^{-.25},$$

and $\Delta\phi$ is the angular separation between the peaks and ν is the frequency. This means that the separation of the components will decrease with frequency. If the double peak is thought to be due to the sweeping of a radiation cone across the line of sight of the observer, so that he sees both lobes of radiation, then observation tells us that the higher

frequency radiation must be emitted at smaller angles to the charges trajectory than the lower frequency signals. We also note that the angular width of the pattern is much too wide, being as large as 60^{o} for the lower frequencies. Observed pulse widths are usually around 10^{o} of the pulse period. Further, whereas observations never show double pulse profiles having peaks separated by more than about 40^{o}, the linear acceleration model has separation of lobes of 120^{o}.

The answer to these discrepancies is in the assumption of a constant electric field accelerating the charges. In reality we would expect the field to be a strong function of distance from the surface of the star. If linear acceleration is to be the mechanism to produce the radiation, the electric field will have to influence the charge in such a way so as to accelerate it at a relativistic velocity. In this manner we will get the observed forward beaming effect. On the other hand the angular radiation pattern may be determined by the radiative transfer characteristics of the plasma in the magnetosphere. In the absence of a maser mechanism, which could modify the spectrum and the radiation pattern, linear acceleration due to a constant field does not agree too well with observations of the radiation pattern.

The calculated spectrum of the accelerated charge is somewhat better however. The upper limit on the electric field due to the rotation of the stars magnetic field is 10^{12} V/cm. The actual value is probably quite a bit less than this since this figure is for a vacuum surrounding the star. By fitting the calculated curve with typical spectral data we find similarities if we assume a field strength of 10^{5} V/cm. This field would produce a spectrum which has a spectral index which ranges from -1 to -2.5 from .1 GHz to 10 GHz. This field is quite

reasonable and might be expected as the average field in the region of the magnetosphere where the radiation is produced.

The spectrum does not exhibit the low frequency cutoff which is often observed in the spectra of pulsars. It is thought that this cutoff must be due to the radiation mechanism since it is not exponential in form which would be the case if the absorption of radiation by the plasma was the cause. The low frequency cutoff could be caused by a field which produced a radiation field which increased at a slower rate than our constant field produces and decreased at a faster rate.

In the next section we will take a look at the manner in which the plasma effects the radiation as it passes through the magnetosphere and how it will alter the form of the spectrum.

FOOTNOTES

[1]P. A. Sturrock, Astrophys. Jour. 164, 529 (1971).

[2]M. A. Rudermann and P. G. Sutherland, Astrophys. Jour. 190, 137 (1974).

[3]F. G. Smith, Mon. Not. Roy. Astron. Soc. 149, 1 (1970).

[4]V. L. Ginzburg, V. V. Zheleznyakov and V. V. Zaitsev, Astrophys. Space Sci. 4, 464 (1969).

[5]D. B. Melrose, Astrophys. Jour. 225, 557 (1978).

[6]H. Heintzmann and J. Nitsch, Astron. Astrophys. 74, 263 (1979).

[7]M. J. Rees and J. E. Gunn, Mon. Not. Roy. Astron. Soc. 167, 1 (1974).

[8]I. Lerche, Astrophys. Jour. 159, 229 (1970).

[9]R. N. Manchester and J. H. Taylor, Pulsars (Freeman and Co., San Francisco, 1977), p. 59.

[10]J. D. Jackson, Classical Electrodynamics (John Wiley and Sons, New York, 1962), Chapter 11.

[11]V. V. Zheleznyakov and V. E. Shaposhnikov, Astrophys. Space Sci. 18, 141 (1972).

[12]F. G. Smith, op. cit.

[13]V. L. Ginzburg, et al., op. cit.

[14]S. Hinata and A. E. Jackson, Astrophys. Jour. 206, 703 (1974).

[15]P. Goldreich and W. H. Goldreich, Astrophys. Jour. 159, 869 (1969).

[16]P. A. Sturrock, op. cit.

[17]P. Goldreich and D. A. Keeley, Astrophys. Jour. 170, 463 (1971).

[18]M. N. Rudermann and P. G. Sutherland, op. cit.

[19]H. Y. Chiu and V. Vanuto, Astrophys. Jour. 163, 577 (1971).

[20]S. A. Kaplan and V. Ya. Eidmann, Sov. Astron. 15, 344 (1971).

[21]W. J. Cocke, Astrophys. Jour. 184, 291 (1973).

[22]D. B. Melrose, op. cit.

[23]L. D. Landau and E. M. Lifshitz, The Classical Theory of Fields, (Pergamon Press, New York, 1975), Chapter 1.

[24]R. D. Sard, Relativistic Mechanics, (W. A. Benjamin, New York, 1970).

[25]J. D. Jackson, Classical Electrodynamics, (John Wiley and Sons, Inc., New York, 1962), Chapter 14.

[26]Ibid.

CHAPTER IV

RADIATIVE TRANSFER

Before the radiation from the emitting region of the pulsar can reach us, it must pass through the plasma surrounding the star. This plasma may have a frequency dependent effect on the transmission of the radiation, which would alter the shape of the spectrum and change the polarization pattern. The transmission properties might also be angle dependent, which could change the beaming pattern of the radiation. This part of our work will make a study of the transmission properties of the plasma and show where they could have an effect on the observed radiation characteristics.

The manner in which the plasma filters the signal is highly dependent on the orientation of the signal's fields with respect to the plasma fields and velocities. This is due to the angular dependence of the velocity-dependent term in the Lorentz force, $\vec{V} \times \vec{B}$, and the relativistic effects which would be expected when the plasma travels at relativistic velocities. For this reason the model of the magnetosphere which we use is very important in determining the transfer function for the radiation. The model which we have proposed is one in which the charge separated plasma streams along the very strong poloidal magnetic field of the star at highly relativistic velocities. The observed radiation is beamed along the magnetic field so that its wave vector is at a small angle to both the velocity of the plasma and the magnetic field.

The interaction between particles is also expected to be angle dependent due to the magnetic field. For fields of the order of 10^{12} Gauss and particle densities of 10^{12} cm^{-3} we know that the Larmor radius for relativistic electrons is

$$r_L = \frac{m\ v\ c}{e\ B} \cong 10^{-9}\ cm, \tag{1}$$

whereas the average particle separation is 10^{-4} cm. This means that the interaction between particles perpendicular to the magnetic field is negligible. The interaction between particles parallel to the magnetic field is probably much greater, allowing for shock waves which have been proposed. The particle separation and the relativistic velocity of the plasma as a whole suggest that we can ignore collisions in calculating the equation of motion for the electron gas as a first approximation. These conditions hold for most polar cap models and so would be applicable to other models of radiation generation.

We will first review the manner in which dispersion relations are calculated for a plasma.

Dispersion Relations

As a radiation field passes through a plasma the radiation fields will interact with the charged particles accelerating them. This acceleration will in turn produce fields which in turn modify the radiation. The resultant radiation modes transferred by the plasma may be found from the dispersion relation for the plasma. This expression relates the frequency, ω of the Fourier components of the signal to its wavevector, k. By finding an expression for the wave vector "k" as a function of frequency we can tell whether the signal will be transmit-

ted, reflected or absorbed by the plasma. The wave vector "k" may be complex so $k = k_{Re} + i\, k_{Im}$ is substituted in the plane wave expression

$$E = E_o\, e^{i(\vec{k}\cdot\vec{x} - \omega t)} \quad . \tag{2}$$

This will give an exponential decay for the imaginary part of the wave-vector.

The study of this interaction between the fields and charged particles is an important part of plasma physics. Plasma physics takes the equations which deal with many-body systems and combines them with the equations which deal with the interactions between electromagnetic fields and charges. It then attempts to solve the equations simultaneously to give a description of the system. This problem is very complicated due to its non-linear nature, i.e., the fields producing alterations in the position and velocity distributions of the charges which in turn alter the fields. The normal approach to this problem is to assume that the fields produce only a small disturbance to the equilibrium configuration and then linearize the equations, ignoring the second order interactions.

The many-body theory used to describe the system is usually hydrodynamics or statistical mechanisms. The hydrodynamical approach is actually a special case of the statistical mechanical approach which assumes the system is in thermodynamic equilibrium so that the distribution function is Maxwellian. The magnetohydrodynamical approach in the one used here. We take this approach because of the lack of interactions perpendicular to the magnetic field and the expected low temperature. The theory treats the interactions of a number of species of charged particles, e.g. electrons and protons, with both static and time

dependent electromagnetic fields.

The equations describing the non-relativistic fluid approach are the equations of motion of the charged species i, i = 1,2, ..., N,

$$m_i \rho_i \{\frac{\partial \vec{v}_i}{\partial \varepsilon} + (\vec{v}_i \cdot \vec{\nabla}) \vec{v}_i\} = e_i \rho_i \{\vec{E}_i + \frac{\vec{v}_i}{c} \times \vec{B}\} - \vec{\nabla} p_i - m_i \rho_i \nu_i \vec{v}_i) \tag{3}$$

the equation of continuity ignoring a sink term, which indicates the recombination of charges

$$\frac{\partial \rho_i}{\partial t} + \vec{\nabla} \cdot (\rho_i \vec{v}_i) = 0, \tag{4}$$

Maxwell's equations

$$\begin{aligned} \vec{\nabla} \cdot \vec{E} &= 4\pi \sum_i^N e_i \rho_i \qquad \vec{\nabla} \times \vec{E} = -\frac{1}{c} \frac{\partial \vec{B}}{\partial t}, \\ \nabla \cdot B &= 0 \qquad \vec{\nabla} \times \vec{B} = \frac{4\pi}{c} \sum_i^N e \rho_i \vec{v}_i + \frac{1}{c} \frac{\partial \vec{E}}{\partial t}, \end{aligned} \tag{5}$$

and the equation of state for the different charged species

$$P_i = C_i m_i \rho_i^{\gamma_i} \tag{6}$$

where i refers to the i^{th} species, e_i and m_i refer to the charge and mass of the components of the plasma, $\vec{v}_i$ is the velocity of the plasma, p_i and ν_i are the partial pressure and the collision rates for the i^{th} species of the plasma, $\vec{E}$ and $\vec{B}$ are the electric and magnetic fields in the plasma and γ_i is the ratio of specific heats at constant pressure and constant volume for the species of the plasma. The expression on the left side of the equation of motion is the convective derivative

which gives the time rate of change of the velocity of a volume element of the plasma at a fixed point in the plasma rather than the derivative of the velocity of a fluid element as it moves through the plasma. Simultaneous solution of these equations specifies the state of the plasma.

As an example of the manner in which the dispersion relations are derived from these equations and as a non-relativistic limit for our calculation we will review the Hartree-Appleton theory for transmission of electromagnetic waves through a magnetoactive plasma.

Hartree-Appleton Equation

The propagation of radio signals in a plasma became of interest in the 1920s when it was noted that short wavelength radiation could be reflected from the ionosphere producing long distance communications links by a process which has come to be known as skip. This problem, which dealt with the propagation of electromagnetic waves through a neutral plasma with an embedded magnetic field due to the Earth's dipole field, was addressed by Hartree[1] and Appleton[2] between 1925 and 1932.

In our treatment we will deal with a neutral plasma with a dissipative component, where the wave vector of the incident radiation is at an angle θ to the B field. The motion of the ions in the plasma will be ignored due to their large mass as compared to the electrons. We will also assume a diffuse plasma with a low temperature so that we may ignore the pressure gradient term in the equation of motion. Since we are dealing with a neutral plasma we have constant charge density so that the continuity equation is trivial. This leaves the Maxwell's equations and the equation of motion to define the fields and the

velocity of the electrons in the plasma.

The method of solution of these equations is to first assume that the values of E, B, v and ρ are not changed very much from their equilibrium values by the passage of the radiation fields. We, therefore, treat these variables as if they consist of a steady state part and a perturbation so

$$\begin{aligned} \vec{E} &= \vec{E}_o + \vec{E}_1 \qquad \rho = \rho_o + \rho_1 \\ \vec{B} &= \vec{B}_o + \vec{B}_o \qquad \vec{\mathbf{v}} = \vec{\mathbf{v}}_o + \vec{\mathbf{v}}_1 \end{aligned} \tag{7}$$

where the subscripts "O" and "1" refer to the steady state and the perturbed parts of the variables, respectively. For our problem there is no steady state field or velocity and the density is a constant so E_o, v_o and ρ_1 are zero. Substituting these expressions into the equation of motion for the electron gives

$$\frac{\partial \vec{v}_1}{\partial t} + (\vec{v}_1 \vec{\nabla}) \vec{v}_1 = \frac{e}{m} \vec{E}_1 + \frac{e}{m} \left[\frac{\vec{v}_1}{c} \times \vec{B}_o + \frac{\vec{v}_1}{c} \times \vec{B}_1 \right] - \nu \vec{v}_1 . \tag{8}$$

The next step is to linearize the equations by dropping terms which are second order in the perturbed quantities which gives

$$\frac{\partial \vec{v}_1}{\partial t} = \frac{e\vec{E}_1}{m} + \frac{e}{mc} \vec{v}_1 \times \vec{B}_o - \nu \vec{v}_1 . \tag{9}$$

This gives an equation which relates the perturbed electric field and velocity of a volume element of the plasma. From Maxwell's equations we derive the wave equation in the usual manner to give another expression relating the field and velocity vectors of the plasma. Using the expression for current

$$\vec{J}_1 = \rho_o e \vec{v}_1, \tag{10}$$

we have the wave equation

$$\vec{\nabla}(\vec{\nabla}\cdot\vec{E}_1) - \nabla^2\vec{E}_1 = \frac{-4\pi}{c^2} e\rho \frac{\partial \vec{v}_1}{\partial t} - \frac{1}{c^2}\frac{\partial^2 \vec{E}_1}{\partial t^2} . \tag{11}$$

These two vector equations relate the components of the perturbed electric fields and velocities in a fluid element of the plasma. The solution to these equations defines the state of the plasam.

We first chose a convenient geometry to describe the system where the steady state magnetic field B_o lies along the z axis and the wave-vector of the radiated field is at an angle θ with respect to B field and lies in the x-z plane.

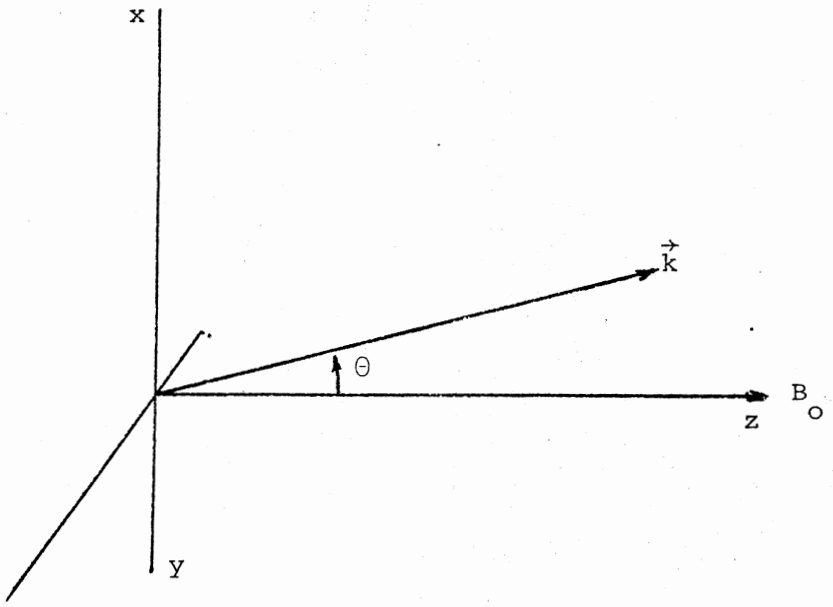

To solve the differential equations we assume that the solutions may be

expressed as Fourier transforms in space and time. We have the transforms

$$F_{x,t}[\vec{E}(\vec{x},t)] = \vec{E}(\vec{k},\omega) = \frac{1}{2\pi}\int_{-\infty}^{\infty} d\vec{x}\int_{-\infty}^{\infty} dt\, E(x,t)e^{-i(\vec{k}\cdot\vec{x}-\omega t)}$$

$$F_{x,t}[\vec{v}(x,t)] = \vec{v}(\vec{k},\omega) = \frac{1}{2\pi}\int_{-\infty}^{\infty} d\vec{x}\int_{-\infty}^{\infty} dt\, v(x,t)e^{-i(\vec{k}\cdot\vec{x}-\omega t)}\ , \tag{12}$$

and the inverse transforms

$$F_{k,\omega}[\vec{E}(k,\omega)] = \vec{E}(\vec{x},t) = \int_{-\infty}^{\infty} d\vec{k}\int_{-\infty}^{\infty} d\omega\, \vec{E}(k,\omega)e^{i(\vec{k}\cdot x-\omega t)}$$

$$F_{k,\omega}[v(k,\omega)] = \vec{v}(\vec{x},t) = \int_{-\infty}^{\infty} d\vec{k}\int_{-\infty}^{\infty} d\omega\, \vec{v}(\vec{k},\omega)e^{i(k\cdot x-\omega t)}\ . \tag{13}$$

The transform of a time derivative of the E field and velocity give the expressions

$$F_{x,t}\left[\frac{\partial\vec{E}}{\partial t}\right] = -i\omega\vec{E}(\vec{k},\omega),\ F_{x,t}\left[\frac{\partial\vec{v}}{\partial t}\right] = -i\omega\vec{v}(\vec{k},\omega), \tag{14}$$

and the transform of the vector operator acting on the E field gives

$$F_{x,t}[\nabla^2\vec{E}] = -k^2\vec{E}(k,\omega);\ F_{x,t}[\vec{\nabla}(\vec{\nabla}\cdot\vec{E})] = -\vec{k}(\vec{k}\cdot\vec{E}) \tag{15}$$

Taking the Fourier transform of the equation of motion and the wave equation we get two algebraic equations in k and ω relating the Fourier components of the E field and the velocity of the plasma. The equation of motion is

$$-i\omega\vec{v}_1 + \nu\vec{v}_1 = \frac{e\vec{E}_1}{m} + \frac{e}{mc}\vec{v}_1 \times \vec{B}_o, \tag{16}$$

and the wave equation becomes

$$-\vec{k}(\vec{k}\cdot\vec{E}) + k^2\vec{E}_1 = \frac{4\pi e\rho}{c^2} i\omega\vec{v}_i + \frac{\omega^2}{c^2}\vec{E}_1 , \qquad (17)$$

where $\vec{E}$ and $\vec{v}$ are functions of the wave vector and the angular frequency. The equation of motion may be decomposed into three vector component equations and solved for the velocity components giving the expressions

$$v_x = \frac{(\omega+i\nu)}{[(\omega+i\nu)^2 - \omega_B^2]} \frac{ieE_x}{m} - \frac{\omega_B}{[(\omega ri\nu)^2 - \omega_B^2]} \frac{eE_y}{m} ,$$

$$v_y = \frac{(\omega+i\nu)}{[(\omega+i\nu)^2 - \omega_B^2]} \frac{ieE_y}{m} + \frac{\omega_B}{[(\omega+i\nu)^2 - \omega_B^2]} \frac{eE_y}{m} , \qquad (18)$$

$$v_z = \frac{i}{(\omega+i\nu)} \frac{eE_z}{m} ,$$

where the cyclotron frequency ω_B is given by

$$\omega_B = \frac{eB}{mc} . \qquad (19)$$

These equations relate the components of the electric field to the components of the velocities of the electron fluid.

By using the wave equation for the electric field in a charged medium we can write three more relations between the fields and the velocities giving a complete set. Normally the wave vector is perpendicular to the electric field so that the $\vec{k}\cdot\vec{E}$ term is zero. In this case, however, the oscillatory motion of the electrons along the wave vector give rise to an electric field component parallel to the wave vector. The wave equation then gives us the three equations

$$-c^2h^2(E_x \sin^2\theta + E_z \cos\theta \sin\theta) + (c^2h^2-\omega^2)E_x = 4\pi e\rho i\omega v_x ,$$

$$(-c^2k^2-\omega^2)E_y = 4\pi e\rho i\omega v_y , \tag{20}$$

and

$$-c^2h^2(E_x \sin\theta \cos\theta + E_z \cos^2\theta) + (c^2k^2-\omega^2)E_z = 4\pi e\rho i\omega v_z .$$

By substituting the expressions for the velocity components in the wave equations we arrive at three equations relating the components of the electric field. Making the substitutions

$$Y = \frac{\omega_B}{\omega} \qquad S = 1 - \frac{X\,U}{U^2 - Y^2}$$

$$X = \frac{\omega_p^2}{\omega^2} \qquad T = 1 - \frac{X}{U} \tag{21}$$

$$U = 1 + \frac{i\nu}{\omega} \qquad D = -\frac{X\,Y}{U^2 - Y^2}$$

and defining the index of refraction

$$n = \frac{c}{v_p} = \frac{c\,k}{\omega} , \tag{22}$$

we arrive at the matrix equation

$$\begin{pmatrix} n^2\cos^2\theta - S & iD & -n^2\sin\theta\cos\theta \\ -iD & h^2 - S & 0 \\ -n^2\cos^2\theta\sin\theta & 0 & n^2\sin^2\theta - T \end{pmatrix} \begin{pmatrix} E_x \\ E_y \\ E_z \end{pmatrix} = 0 \ . \quad (23)$$

For the fields to be non-zero the determinant must be zero. This gives the equation

$$n^2(T\cos^2\theta + S\sin^2\theta) + n^2[TS(1+\cos^2\theta) + (S^2-D^2)\sin^2\theta] + T(D^2-S^2) = 0 \quad (24)$$

which is quadratic in n^2. Solving for n^2 we get the expression

$$n^2 = 1 - \frac{X}{U - \frac{Y^2\sin^2\theta}{2(U-X)} \pm \left[\frac{Y^4\sin^4\theta}{4(U-X)^2} + Y^2\cos^2\theta\right]^{\frac{1}{2}}} \ , \quad (25)$$

as the dispersion relation for radiation traveling through a neutral plasma whose magnetic field makes an angle θ to the wave vector of the radiation. From this equation we see that we get the condition for reflection, $n = 0$, when

$$T^2(D^2 - S^2) = 0 \ , \quad (26)$$

or equivalently

$$X = 1, \quad X = 1 - Y, \quad \text{or} \quad X = 1 + Y \ , \quad (27)$$

giving us the cut off frequencies of

$$\omega_o = \omega_p; \quad \omega = \frac{\pm \omega_B \pm \sqrt{\omega_B^2 + 4\omega_p^2}}{2} . \tag{28}$$

Note that the cut off frequency is independent of the angle of propagation. The various cut off frequencies correspond to the modes of propagation corresponding to ordinary and extraordinary waves and left and right polarization.

The resonances in the plasma occur when the phase velocity of the wave goes to zero or, equivalently the index of refraction goes to infinity. In this case the coefficient of the fourth order term must be zero. From the determinant's characteristic equation we find the angle dependent expression for the resonance

$$\tan^2\theta = -\frac{T}{S} = -1 + \frac{\omega_p^2\omega_B^2}{\omega^4 - \omega_p^2\omega^2 - \omega_B^2\omega^2} . \tag{29}$$

From this we find the standard results for the propagation across the steady state magnetic field

$$\omega = \sqrt{\omega_B^2 + \omega_p^2} \quad \text{the ordinary wave} \tag{30}$$

and propagation parallel to the B field

$$\omega = \omega_B \quad \text{the extraordinary wave.} \tag{31}$$

Relativistic Treatment of Dispersion Relations

Note that the previous treatment did not deal with the magnetic radiation field, B_1. This was due to the fact that the particle

velocity in the unperturbed plasma was zero or very low and the second order terms were dropped. For the case of plasmas which move at relativistic speeds the $\frac{v_o}{c} \times B_1$ term in the equation of motion becomes significant and the radiation field B_1 must be included in the treatment. This section of the study will look at the way in which relativistic effects are treated.

In passing it should be noted that a number of recent treatments of this problem are inconsistent.[3,4] The line of attack used in these works was to solve the problem in the rest frame of the plasma and then transform to a system at rest. This will have the effect of Doppler shifting the frequency of the radiation, increasing the density of the plasma due to Lorentz contraction, and increasing the mass of the electrons. The usual treatment then was just to substitute the Lorentz transformed expressions in for these parameters in the non-relativistic expression. This approach, however, ignores the fact that the fields in the original derivation are also transformed since they have components which are transverse to the direction of motion.

The manner in which we approach the problem looks at it from the laboratory frame of reference. In this case the equation of motion for a charge moving at relativistic speeds is

$$\frac{d}{dt}\left(\frac{\vec{mv}}{\sqrt{1 - v^2/c^2}}\right) = e(\vec{E} + \frac{\vec{v}}{c} \times \vec{B}), \qquad (32)$$

where we ignore the pressure and collisional terms from the non-relativistic expression. This means that we are ignoring particle interactions.

For the hydrodynamical approach we wish to observe the interaction of a volume element of the plasma rather than following a volume element

through the plasma. For this reason we use the convective form for the derivative of momentum

$$m_o \frac{d}{dt}(\gamma\vec{v}) = \frac{\partial}{\partial t}(\gamma\vec{v}) + \vec{v}\cdot\vec{\nabla}(\gamma\vec{v}) \tag{33}$$

where

$$\gamma = \frac{1}{\sqrt{1 - v^2/c^2}} .$$

Expanding this expression we get the equation of motion as

$$\vec{v}\frac{\partial\gamma}{\partial t} + \gamma\frac{\partial\vec{v}}{\partial t} + \vec{v}(\vec{v}\cdot\vec{\nabla}\gamma) + \gamma(\vec{v}\cdot\vec{\nabla})\vec{v} = \frac{e}{m_o}(\vec{E} + \frac{\vec{v}}{c} \times \vec{B}) . \tag{34}$$

Again we treat the variables of the problem as if they are only slightly disturbed from equilibrium so that they are expanded in a large steady state component and a small perturbed contribution, eq. 7. Substituting these expressions in for the variables v, E and B we have the expression

$$(\vec{v}_o+\vec{v}_1)\frac{\partial\gamma}{\partial t} + \gamma\frac{\partial}{\partial t}(\vec{v}_o+\vec{v}_1) + (\vec{v}_o+\vec{v}_1)[(\vec{v}_o+\vec{v}_1)\cdot\vec{\nabla}\gamma]$$

$$+ \gamma[(\vec{v}_o+\vec{v}_1)\cdot\vec{\nabla}(\vec{v}_o+\vec{v}_1)] = \frac{e}{m_o}[\vec{E}_1 + \frac{(\vec{v}_o+\vec{v}_1)}{e} \times (\vec{B}_o+\vec{B})] . \tag{35}$$

The relativistic factor γ is also a function of the velocities $\vec{v}_o+\vec{v}_1$

$$\gamma = \frac{1}{\sqrt{1 - \frac{(v_o+v_1)^2}{c^2}}} = \frac{1}{\sqrt{1 - \frac{v_o^2 + 2\vec{v}_o\cdot\vec{v}_1 + v_1^2}{c^2}}} . \tag{36}$$

Since v_o is a constant in time the derivative of γ is

$$\frac{\partial \gamma}{\partial t} = \gamma^3 \frac{(\vec{v}_o+\vec{v}_1)}{c^2} \cdot \frac{\partial \vec{v}_1}{\partial t} , \tag{37}$$

and the space derivative term of γ is

$$(\vec{v}_o+\vec{v}_1)\cdot\vec{\nabla}\gamma = \gamma^3(\vec{v}_o+\vec{v}_1) \cdot \left(\vec{\nabla}\left[\frac{\vec{v}_o \cdot \vec{v}_1}{c^2}\right] + (\vec{\nabla}\vec{v}_1) \cdot \frac{\vec{v}_1}{c^2}\right) . \tag{38}$$

The full expanded version of the convective derivative of $\gamma\vec{v}$ is

$$\gamma^3 \frac{\vec{v}_o}{c^2} v_o \cdot \frac{\partial \vec{v}_1}{\partial t} + \gamma^3 \frac{\vec{v}_o}{c^2} \vec{v}_1 \cdot \frac{\partial \vec{v}_1}{\partial t} + \gamma^3 \frac{\vec{v}_1}{c^2} \vec{v}_o \cdot \frac{\partial \vec{v}_1}{\partial t} + \Gamma^3 \frac{\vec{v}_1}{c^2} \vec{v}_1 \cdot \frac{\partial \vec{v}_1}{\partial t}$$

$$+ \gamma \frac{\partial \vec{v}_1}{\partial t} + \gamma^3 \vec{v}_o[\frac{\vec{v}_o}{c^2} \cdot \vec{\nabla}(\vec{v}_o\cdot\vec{v}_1)] + \gamma^3 \vec{v}_o [\frac{\vec{v}_o}{c^2} \cdot (\vec{\nabla}\vec{v}_1)\cdot\vec{v}_1]$$

$$+ \gamma^3 \vec{v}_o[\frac{\vec{v}_1}{c^2} \cdot \vec{v}(\vec{v}_o\cdot\vec{v}_1)] + \gamma^3 \vec{v}_o[\frac{\vec{v}_1}{c^2} \cdot (\vec{\nabla}\vec{v}_1)\cdot\vec{v}_1] \cdot \gamma^3 \vec{v}_1[\frac{\vec{v}_o}{c^2} \cdot \vec{\nabla}(\vec{v}_o\cdot\vec{v}_1)]$$

$$+ \gamma^3 \vec{v}_1[\frac{\vec{v}_o}{c^2} \cdot (\vec{\nabla}v_1)\cdot\vec{v}_1] + \gamma^3 \vec{v}_1[\frac{\vec{v}_1}{c^2} \cdot \vec{\nabla}(\vec{v}_o\cdot\vec{v}_1)] + \gamma^3 \vec{v}_1[\vec{v}_1\cdot(\vec{\nabla}\vec{v}_1)\cdot\vec{v}_1]$$

$$+ \gamma\vec{v}_o \cdot \vec{\nabla}\vec{v}_1 + \gamma \vec{v}_1 \cdot \vec{\nabla}\vec{v}_1 . \tag{39}$$

By Fourier transforming the expression for the convective derivative we get an algebraic expression in terms of the wave vector and angular frequency. By dropping the second order terms in the perturbed quantities we get the expression for the linearized equation of motion

$$-i\omega\gamma^3 \frac{\vec{v}_o}{c^2}(\vec{v}_o\cdot\vec{v}_1) - i\omega\gamma\vec{v}_1 + i\gamma^3 \frac{v_o}{c^2}(\vec{v}_o\cdot\vec{k})(\vec{v}_o\cdot\vec{v}_1) + i\gamma(\vec{v}_o\cdot\vec{h})\vec{v}_1$$

$$= \frac{e}{m_o}\vec{E}_1 + \frac{e}{m_o c}\vec{v}_1 \times \vec{B}_o + \frac{e}{m_o c}\vec{v}_o \times \vec{B}_1 \ . \qquad (40)$$

Note that we have set the steady state part of the electric field to zero. We do this since we are dealing with the transfer of the radiation outside of the acceleration zone, where the large electric fields accelerate the charges.

We choose the geometry of the problem so that the wave vector lies in the x-z plane and makes an angle of θ with the steady state components of the velocity and the magnetic field.

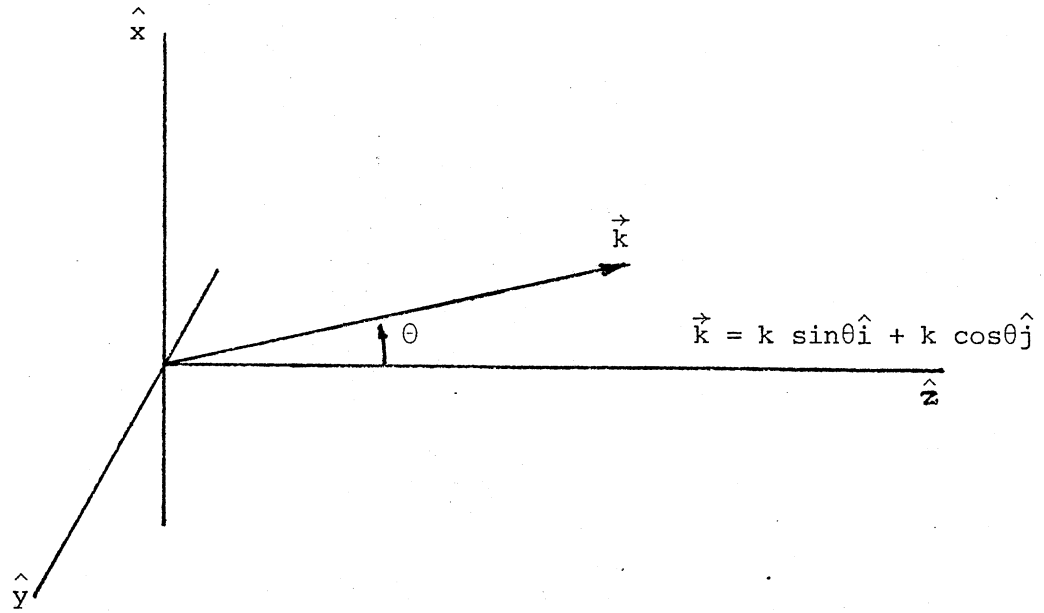

Let $\vec{B}_o = B_o\hat{k}$ and $\vec{v}_o = v_o\hat{k}$ where $\hat{i}$, $\hat{j}$, and $\hat{k}$ are the unit vectors in the x, y, and z directions. We now have the algebraic form for the equation of motion

$$- i\omega\,\gamma^3 \frac{\vec{v}_o}{c^2} v_o v_{1z} - i\gamma\,\omega\vec{v}_1 + i\gamma^3(\vec{v}_o \cdot \vec{h})\frac{\vec{v}_o}{c^2} v_o v_{1z}$$

$$+ i\gamma(\vec{v}_o \cdot \vec{k})\vec{v}_1 = \frac{e}{m}\vec{E}_1 + \frac{e}{m_o c}\vec{v}_1 \times \vec{B}_o + \frac{e}{m_o c}\vec{v}_o \times \vec{B}_1 , \qquad (41)$$

$$\vec{v}_1 \times \vec{B}_o = v_y B_o \hat{i} - v_x B_o \hat{j}; \quad \vec{v}_o \times \vec{B}_1 = -v_o B_y \hat{i} + v_o B_x \hat{j} . \qquad (42)$$

The equation of motion gives us a relationship between the components of the velocity, the electric and the magnetic fields. If we solve the three component equations for the velocity components we get the expressions

$$v_x = \frac{\frac{-ie}{\gamma m}}{(1-\gamma^2)(v_o k\cos\theta-\omega)} (E_x - \beta B_y - iYE_y - iY\beta B_x),$$

$$v_y = \frac{\frac{-ie}{\gamma m}}{(1-\gamma^2)(v_o k\cos\theta-\omega)} (E_y + iYE_x + \beta B_x - iY\beta B_y), \qquad (43)$$

$$v_z = \frac{-ie\, E_z}{\gamma^3 m\,(v_o k\cos\theta-\omega)} ,$$

where

$$Y = \frac{\omega_B}{(v_o k\cos\theta-\omega)}, \quad \beta = \frac{v_o}{c}, \quad \text{and} \quad \omega_B = \frac{eB_o}{\gamma mc} . \qquad (44)$$

The form of the wave equations relating the electromagnetic fields and the velocities of the charge elements is Lorentz invariant. In the lab frame the wave equations for the electric and magnetic fields have the Fourier transforms

$$-\vec{k}(\vec{k}\cdot\vec{E}) + k^2\vec{E} = \frac{4\pi e\rho}{c^2} i\omega\vec{v} + \frac{\omega^2}{c^2}\vec{E} ,$$

$$-\vec{k}(\vec{k}\cdot\vec{B}) + k^2\vec{B} = \frac{4\pi e\rho}{c^2} i\vec{k} \times \vec{v} + \frac{\omega^2}{c^2}\vec{B} , \tag{45}$$

where the current density has been written in terms of the velocity

$$\vec{J} = e\rho\vec{v} . \tag{46}$$

Expanding the wave equations in their vector components we get six equations which, together with the three velocity component equations, give us a system of nine equations and nine unknowns which may be solved in the usual manner. The wave equations give us the six expressions

$$(c^2k^2\cos^2\theta-\omega^2)E_x - c^2k^2\sin\theta\cos\theta\ E_z = 4\pi\rho ei\omega v_x \quad (c^2k^2-\omega^2)E_y = 4\pi e\rho i\omega v_y$$

$$- c^2k^2\cos\theta\sin\theta + (c^2k^2\sin^2\theta-\omega^2)E_z = 4\pi e\rho i\omega v_z \quad (c^2k^3\cos^2\theta-\omega^2)$$

$$x\ B_x - c^2k^2\sin\theta\sin\theta\ B_z = -4\pi e\rho cik\cos\theta v_y \quad (c^2k^2-\omega^2)B_y = 4\pi e\rho ick(\cos\theta v_y$$

$$- \sin\theta v_z) - c^2k^2\cos\theta\sin\theta\ B_x + (c^2k^2\sin^2\theta-\omega^2)B_z = 4\pi e\pi icksin\theta v_y$$

By substituting in the expressions for the velocity components we can eliminate them from the system of equations giving us six equations dealing with the electric and magnetic fields. These are:

From E_x Equation:

$$(n^2\cos^2\theta-1-S)E_x + iDE_y - n^2\sin\theta\cos\theta\ E_z + iD\beta B_x$$

$$+ \beta SB_y = 0 , \tag{48}$$

From the E_y Equation:

$$-iDE_x + [n^2-1-S]E_y - \beta SB_x + i\beta DB_y = 0 \ , \tag{49}$$

From the E_z Equation:

$$-n^2\cos\theta\sin\theta E_x + (n^2\sin^2\theta-1-T)E_z = 0 \ , \tag{50}$$

From the B_x Equation:

$$iD_n\cos\theta E_x + S_n\cos\theta E_y + (n^2\cos^2\theta-\beta S_n\cos\theta)B_x$$

$$-i\beta D_n\cos\theta\ B_y - n^2\sin\theta\cos\theta\ B_z = 0 \ , \tag{51}$$

From the B_y Equation:

$$-S_n\cos\theta E_x + iD_n\cos\theta E_y + T_n\sin\theta E_z + iD\beta_n\cos\theta B_x + (n^2-1+\beta S_n\cos\theta)B_y = 0 \ , \tag{52}$$

From the B_z Equation:

$$-iD_n\sin\theta E_x - S_n\sin\theta E_y - (n^2\sin\theta\cos\theta + \beta S_n\sin\theta)B_x$$

$$+ iD\beta_n\sin\theta B_y + (n^2\sin^2\theta-1)B_z = 0 \ , \tag{53}$$

where

$$S = \frac{X}{(1-Y^2)(\beta_n\cos\theta-1)} \ , \qquad D = \frac{XY}{(1-Y^2)(\beta_n\cos\theta-1)} \ ,$$

$$T = \frac{X}{\gamma^2(\beta_n\cos\theta-1)}, \qquad X = \frac{\omega\rho^2}{\omega^2}, \qquad \omega_p = \frac{4\pi e^2\rho}{\gamma m} \ , \tag{54}$$

and n is the index of refraction given by

$$n = \frac{c\,k}{\omega} . \tag{55}$$

This system of six equations may be solved simultaneously by evaluating the determinant of the coefficients of the fields. The matrix equation is displayed in Figure 3. This six by six determinant was evaluated using the algebraic manipulative computer program REDUCE.[5] The result is an eighth order polynomial in the index of refraction given by

$$n^8(S\sin^2\theta + T\cos^2\theta + 1) = n^7\beta(\sin^2\theta\cos\theta(S^2-D^2) + ST\cos\theta(1 + \cos^2\theta)$$

$$+ 2S\cos\theta) + n^6(-4 + \sin^2\theta(D^2-S^2) - T(3\cos^2\theta + 1) - S(3\sin^2\theta + 2$$

$$+ST(\cos^2\theta + 1) + \beta\cos^2\theta(\beta(S^2-D^2) - \beta D^2T + ST) + 2n^5\beta\cos\theta(-S^2T)$$

$$- ST(\cos^2\theta + 2) - 3S + TD^2 + D^2(\sin^2\theta + 1)) + n^4(7-D^2(2\sin^2\theta + 1)$$

$$+ 3T(\cos^2\theta + 1) - TD^2 + 3S(\sin^2\theta + 2) + 2ST(\cos^2\theta + 2) + S^2(2\sin^2\theta + 1)$$

$$+ S^2T + 2\cos^2(1 + T)(D^2-S^2)) + n^3\beta\cos\theta(4T(S^2-D^2) + S^2(\sin^2\theta + 4)$$

$$+ ST(\cos^2y + 5) + 2S(\sin^2\theta + 2) - D^2(\sin^2\theta + 3) + n^2(-4 + D^2(\sin^2\theta + 2)$$

$$- T(\cos^2\theta + 2) + 2TD^2 - S(\sin^2\theta + 6) - ST(\cos^2\theta + 5) - 2S - S^2\sin^2\theta$$

$$- 2S^2T + \beta^2(S^2\cos^2\theta(1 + T) - D^2\cos^2\theta)1 + T))) + 2n\beta\cos\theta)1+T)(S^2-D^2+S)$$

$$+ S^2(1 + T) + 2S(1 + T) - D^2(1 + T) + (1 + T) = 0 . \tag{56}$$

$n^2\cos^2\theta-1-S$	iD	$-n^2\sin\theta\cos\theta$	$i\beta D$	βS	0
$-iD$	n^2-1-S	0	$-\beta S$	$i\beta D$	0
$-n^2\cos\theta\sin\theta$	0	$n^2\sin^2\theta-1-S$	0	0	0
$iDn\cos\theta$	$Sn\cos\theta$	0	$n^2\cos^2\theta-1 + Sn\cos\theta$	$i\beta Dn\cos$	$-n^2\sin\theta\cos\theta$
$-Sn\cos\theta$	$iDn\cos\theta$	$Tn\sin\theta$	$i\beta Dn\cos\theta$	$n^2-1\ Sn\cos\theta$	0
$-iDn\sin\theta$	$-Sn\sin\theta$	0	$-n^2\sin\theta\cos\theta$ $-\beta Sn\sin\theta$	$i\beta Dn\sin\theta$	$n^2\sin^2\theta-1$

Figure 3. Determinant for Calculating the Dispersion Relation

As a first check on the validity of the above expression we look at the non-relativistic limit. We first note that the odd orders of n all have a multiplicative factor of β which goes to zero in the non-relativistic limit. Next we see that for the cut-off condition of n = 0 we have the equation

$$(1 + T)(S^2 + 2S + 1 - D^2) = 0 . \tag{57}$$

For the non-relativistic limit the parameters S, D, T and Y become

$$S = \frac{-X}{(1-Y^2)}, \quad D = \frac{-XY}{(1-Y^2)}, \quad T = -X, \quad Y = \frac{-\omega_B}{\omega} \tag{58}$$

Substituting these back into the expression and solving for the frequency we get

$$\omega = \omega_p ; \quad \omega = \frac{\pm \omega_B \pm \sqrt{\omega_B^2 + 4\omega_p^2}}{2} \tag{59}$$

which are the same as the non-relativistic expressions.

The resonant frequencies may be found by investigating the polynomial's behavior for very large n. In this case the leading term becomes important and its coefficient must go to zero for equality to hold. From this requirement we get the equation

$$\tan^2\theta = -\frac{1 + T}{1 - S} \tag{60}$$

Substituting the parameters S and T, the angular dependent resonance expression is

$$\tan^2\theta = -\frac{(\omega^2-\omega_p^2)(\omega^2-\omega_B^2)}{(\omega^2-(\omega_B^2+\omega_p^2))} \tag{70}$$

We give two cases as the principal resonances according to the angle of propagation. We take the case of parallel and perpendicular radiation with respect to the magnetic field which gives us the two resonant frequencies

$$\theta = 0 \qquad \theta = \frac{\pi}{2}$$
$$\text{AND} \tag{71}$$
$$\omega = \omega_B \qquad \omega = \sqrt{\omega_B^2 + \omega_p^2},$$

which are in agreement with the expressions derived in the non-relativistic treatment.

Next we look at the relativistic expressions for the cutoff and resonant frequencies. We again have the cutoff condition $n\to 0$ which leaves only the zeroth order term in the polynomial. This must be zero for equality to hold and from this condition we get the equation

$$(1+T)\left[(S+1)^2 - D^2\right] = 0 \quad . \tag{72}$$

or

$$\left(1 + \frac{\omega_p^2}{\gamma^2\omega^2}\right)\left[\left[\left(1 - \frac{X}{1-Y^2}\right)^2 - \frac{X^2Y^2}{1-Y^2}\right]\right] = 0 \, .$$

This gives the cutoff frequencies as

$$\omega = \frac{\omega_p}{\gamma}, \quad \omega = \frac{\pm\,\omega_B \pm \sqrt{\omega_B^2 + 4\omega_p^2}}{2}, \tag{73}$$

where $\omega_p = (\frac{4\pi e^2 \rho}{\gamma m})^{\frac{1}{2}}$ and $\omega_B = \frac{e\,B}{\gamma mc}$. The resonant frequencies may be found by setting the coefficient of the highest order term in the polynomial equal to zero. Here we must remember that the parameters S, D, T, and Y are also functions of n. As before the resonant frequencies are dependent on the angle of propagation. The parameters S, D, T, and Y become in the limit of very large n

$$\begin{aligned} \theta &= 0 & \qquad \theta &= \frac{\pi}{2} \\ S &= \frac{X}{\beta n} & S &= \frac{-X}{1 - \frac{\omega_B^2}{\omega^2}} \\ T &= \frac{X}{\gamma^2 \beta n} \quad \text{AND} & & \\ D &= \frac{XY}{\beta^2 n^2} & T &= \frac{-X}{\gamma^2} \\ & & D &= \frac{-XY}{1 - \omega_B^2/\omega^2} \end{aligned} \tag{74}$$

The highest order term is

$$(S\sin^2\theta + T\cos^2\theta + 1)n^8 \tag{75}$$

for $\theta = 0$ we get

$$(\frac{T}{\gamma^2 n\beta} + 1)n^8 = n^8 + \frac{T}{\gamma^2 \beta} n^7 \tag{76}$$

The coefficient of the n^8 term is one and the equation cannot be satisfied for the resonant condition $n \to \infty$. For $\theta = \frac{\pi}{2}$ we have

$$(\frac{-X}{1 - \omega_B^2/\omega^2} + 1)n^8 \tag{77}$$

The coefficient goes to zero if

$$\omega = \sqrt{\omega_p^2 + \omega_B^2} \tag{78}$$

where $\omega_p = (\frac{4\pi e^2 \rho}{\gamma m})^{\frac{1}{2}}$ and $\omega_B = \frac{e B}{\gamma mc}$. Thie is just the relativistic version of the resonant condition for the ordinary wave in the non-relativistic treatment.

The parameters describing the pulsar magnetosphere have yet to be fixed with any certainty. In particular the density and the relativistic factor have been given a wide range of values in various articles. A density of 10^{12} cm is most often cited in the literature as being the expected value due to the redistribution of the electric charges under the action of the electric field. The relativistic factor is given values of between 10 and 1000 for the various polar cap radiation mechanisms. A value of 10^8 V/m for the electric field would give a value of 10 for the relativistic factor. This would correspond to an acceleration of the electron over a distance corresponding to the radius of the polar cap, i.e. 100 m. Given these parameters we get values for the plasma and cyclotron frequencies of

$$\omega_p = 2 \times 10^{16} \text{ RAD/SEC} \qquad \omega_B = 2 \times 10^{18} \text{ RAD/SEC}$$

Substituting these in our expressions for the cutoff frequencies we get

$$f \cong 300 \text{ MHz}, \quad f = 3 \times 10^{11} \text{ MHz}, \quad f = 200 \text{ Hz}$$

for the three modes of propagation. The cutoff at 300 MHz seems to be a reasonable match for the observed cutoff frequency.

The region where the charges produce the radiation is also an unknown factor. For the polar cap model which we are using it must be within the light cylinder. This region extends from the surface of the star to a distance of 10^5 m to 10^7 m depending on the period of rotation of the star. If the radiation takes place in the upper atmosphere, significantly far away from the star, the magnetic field strength will decrease as the inverse cube of the distance. This could mean that the field strength of the magnetic field would be as small as 10^6 Gauss in the region through which the radiation passed. A reduction of the cyclotron frequency would produce a reduction in the cutoff frequency of the circular mode of radiation. Substitution of a value of 10^6 in the expression for the cyclotron frequency gives a cutoff frequency for the left-handed circularly polarized radiation of the order of 100 MHz.

Summary

The impetus for this section of the work was the prevalent belief that the cutoff frequency would not be due to the radiation transfer through the plasma. Because of this belief those researchers developing a radiation mechanism were charged with the responsibility of producing a spectrum which had a low frequency cutoff. Although theories postulating absorption by plasma bunches have been advanced the state of these theories is not much beyond the qualitative stage. Showing that the cutoff may indeed be due to a low cutoff frequency of the plasma takes this burden off the radiation mechanism theories. By using the observed cutoff frequencies and the expressions given by the relativistic theory, we may be able to fix the value of the density, the relativistic factor, which is related to the electric field, and perhaps the

magnetic field strength in the region through which the radiation passes, which is related to the distance from the star. These values of the parameters describing the pulsar may be used in the radiation mechanism theories to produce a more self-consistent model for pulsars.

FOOTNOTES

[1]E. V. Appleton, Proc. Phys. Soc. 37, 16D (1925); Nature 135, 618 (1935).

[2]D. R. Hartree, Proc. Camb. Phil. Soc. 25, 97 (1929); 27, 143 (1931).

[3]H. Unz and B. R. Chawla, Electromagnetic Waves in Moving Magnetic Plasmas, (University of Kansas Press, Lawrence, 1971).

[4]M. Elitzur, Astrophys. Jour. 190, 673 (1974).

[5]A. C. Hearn, Reduce II (University of Utah, 1973).

CHAPTER V

RADIATION COHERENCE AND PLASMA SHOCKS

As has been mentioned previously the radiation emitted by pulsars must be coherent in order to explain its intensity. The two mechanisms used to explain this coherence are localization of the emission region by bunching of the radiating charge and amplification of the signal by a maser action. The mechanism studied here is the shock wave or bunching model.

Sturrock was first to suggest coherence by bunching when he noted that the flow of plasma from the surface of the star would not be expected to be steady.[1] This suggestion was followed a year later by his charge sheet model in which cascades of electron-positron pairs produced localizations of charges flowing along the magnetic field lines. Goldreich and Keeley noted the similarity between the trajectories of the charges traveling along the curved magnetic field lines of the star and the path that electrons take in a synchrotron.[2] The electrons in a synchrotron are unstable to bunching due to the radiation reaction of the synchrotron radiation they produce. Using this same mechanism bunching of the charges following the magnetic field lines was postulated. Rudermann and Sutherland used Sturrock's model which produced electron-positron pairs with vastly different velocities to suggest a two-stream instability was the source of the bunching for the charges.[3] In this section of the work we are interested in the effect that the supersonic

flow of the plasma could have on the stability of the currents along the magnetic field lines of a neutron star.

Theory of Shocks

In fluid mechanics the study of shock waves originated with the analysis of waves of finite amplitude propagating in a medium where the fluid velocity is supersonic, i.e., exceeding the speed of an acoustic wave in it. The existence of a shock essentially means discontinuities in pressure, density and velocity on either side of the front and these must satisfy the "jump" relations first established by Rankine and Hugoniot. The fundamental physical principles on which these relations are based are conservation of mass flow, conservation of momentum and conservation of energy and these in turn can be derived from the continuity equation, the equation of motion and the energy equation.[4] Taking the x axis of a rectangular coordinate system parallel to the direction of a one-dimensional viscous flow the steady state equations of continuity, motion and energy are respectively

$$\frac{\partial}{\partial y}(\rho v) = 0$$

$$\rho v \frac{\partial v}{\partial x} = -\frac{\partial p}{\partial x} + \frac{4}{3}\frac{\partial}{\partial y}(\mu \frac{\partial v}{\partial x})$$

$$\frac{\partial}{\partial x}\{\rho v(\frac{1}{2}v^2 + h) - \frac{4}{3}\mu v \frac{\partial v}{\partial x} - \lambda \frac{\partial T}{\partial x}\} = 0$$

Here ρ is the density of the fluid, v its velocity, $\rho v = \mu$ the coefficient of viscosity, λ the coefficient of thermal conductivity and h the enthalpy. By integrating these through the shock front, a procedure somewhat akin to deriving matching conditions across boundaries in

electromagnet theory, one obtains the equations

$$\rho_1 v_1 = \rho_2 v_2$$

$$\rho_1 v_1^2 + P_1 = \rho_2 v_2^2 + P_2$$

$$\frac{1}{2} v_1^2 + h_1 = \frac{1}{2} v_2^2 + h_2$$

where the number subscripts refer to the side of the shock as shown below

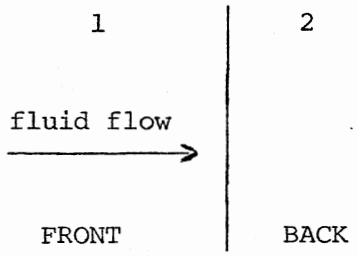

Thermodynamic considerations require that the entropy increases across the shock as also the pressure. The above relations were derived on the basis that outside the shock layer and far from it the motion is steady and uniform.

Hoffmann and Teller were the first to investigate magneto-hydrodynamic shocks where the fluid is a conducting plasma in an external magnetic field.[5] They discussed parallel and perpendicular shocks, i.e. shocks where the direction of propagation is parallel or perpendicular to the magnetic lines of force, a distinction that does not exist in hydrodynamics. Here we have a charged conducting fluid, an elastic continuum, interacting with a given external electromagnetic field governed by Maxwell's equations. The general motion is then described in terms of the stress-energy tensor of the fluid and the energy-momentum tensor of the electromagnetic fields, especially because one is dealing with

general energy momentum conservation laws. It is well known in the mechanics of elastic continua as well as the Maxwell's theory of the electromagnetic field that the kinematical characteristics and the equations of motion are built in the symmetry and divergence properties of these tensors. Furthermore the tensor formulation has the advantage of relativistic generalization because the transformation properties of these tensors with respect to Lorentz transformations are very straightforward. The four-dimensional stress energy tensor of the elastic continuum $\theta_{\mu\nu}$ and the energy momentum tensor of the electromagnetic field $S_{\mu\nu}$ are given in Figure 4.

An elegant point in the Teller derivation is to choose a coordinate system in which the shock front is at rest thus making the system time-independent and then Lorentz transform the usual flow quantities to this rest system. Another simplification in their derivation is that the electric field is taken to be zero, in other words the conductivity is taken to be very high in this case. The stress-energy tensor of the continuum reduces to a simple pressure tensor with diagonal components only in the case of a conducting fluid. The basic Lorentz transformation and tensor transformations are given below as also in Figure 5 in their matrix form. Hoffmann and Teller were able to deduce the relativistic Rankine-Hugoniot relations, in the case of parallel shocks, by simply using the requirement that the four-dimensional divergence of the total stress energy equation $T_{\mu\nu}$ vanishes

$$T_{\mu\nu} = \theta_{\mu\nu} + S_{\mu\nu}; \qquad \frac{d\, T_{\mu\nu}}{dx^{\nu}} = 0$$

and also that Maxwell's equations are to be satisfied in any frame of

$$S_{ik} = \begin{pmatrix} -\tfrac{1}{2}(E_x^2 - E_y^2 - E_z^2 + H_x^2 - H_y^2 - H_z^2) & -(E_xE_z + H_xH_y) & -(E_xE_z + H_xH_z) & i(E_yH_z - E_zH_y) \\ -(E_yE_x + H_zH_x) & -\tfrac{1}{2}(-E_x^2 + E_y^2 - E_z^2 - H_x^2 + H_y^2 - H_z^2) & -(E_yE_z + H_yH_z) & i(E_zH_x - E_xH_z) \\ -(E_zE_x + H_zH_x) & -(E_zE_y + H_zH_y) & -\tfrac{1}{2}(-E_x^2 - E_y^2 + E_z^2 - H_x^2 - HH_y^2 + H_z^2) & i(E_xH_y - E_yH_x) \\ i(E_yH_z - E_zH_y) & i(E_zH_x - E_xH_z) & i(E_xH_y - E_yH_x) & -\tfrac{1}{2}(E^2 + H^2) \end{pmatrix}$$

$$\theta_{ik} = \begin{pmatrix} \gamma^2\mu_o u_x u_x & \gamma^2\mu_o u_x u_y & \gamma^2\mu_o u_x u_z & \gamma^2\mu_o u_x(ic) \\ \gamma^2\mu_o u_y u_x & \gamma^2\mu_o u_y u_y & \gamma^2\mu_o u_y u_z & \gamma^2\mu_o u_y(ic) \\ \gamma^2\mu_o u_z u_x & \gamma^2\mu_o u_z u_y & \gamma^2\mu_o u_z u_z & \gamma^2\mu_o u_z(ic) \\ \gamma^2\mu_o u_x(ic) & \gamma^2\mu_o u_y(ic) & \gamma^2\mu_o u_z(ic) & \gamma^2\mu_o(ic)(ic) \end{pmatrix}$$

$$\gamma = \frac{1}{\sqrt{1 - \mu^2/c^2}}$$

μ_o = rest mass of charge

Figure 4. Energy-Momentum Tensor θ_{ik} and Electromagnetic Energy-Momentum Tensor S_{ik}

$$
\begin{bmatrix}
\gamma^2 & 0 & 0 & -\gamma^2\beta & 0 & 0 & 0 & 0 & 0 & 0 & 0 & 0 & -\gamma^2\beta & 0 & 0 & \gamma^2\beta^2 \\
0 & \gamma & 0 & 0 & 0 & 0 & 0 & 0 & 0 & 0 & 0 & 0 & 0 & -\gamma\beta & 0 & 0 \\
0 & 0 & \gamma & 0 & 0 & 0 & 0 & 0 & 0 & 0 & 0 & 0 & 0 & 0 & -\gamma\beta & 0 \\
-\gamma^2\beta & 0 & 0 & \gamma^2 & 0 & 0 & 0 & 0 & 0 & 0 & 0 & 0 & \gamma^2\beta^2 & 0 & 0 & -\gamma^2\beta \\
0 & 0 & 0 & 0 & \gamma & 0 & 0 & -\gamma\beta & 0 & 0 & 0 & 0 & 0 & 0 & 0 & 0 \\
0 & 0 & 0 & 0 & 0 & 1 & 1 & 0 & 0 & 0 & 0 & 0 & 0 & 0 & 0 & 0 \\
0 & 0 & 0 & 0 & 0 & 0 & 0 & 0 & 0 & 0 & 0 & 0 & 0 & 0 & 0 & 0 \\
0 & 0 & 0 & 0 & -\gamma\beta & 0 & 0 & \gamma & 0 & 0 & 0 & 0 & 0 & 0 & 0 & 0 \\
0 & 0 & 0 & 0 & 0 & 0 & 0 & 0 & 0 & 0 & 0 & -\gamma\beta & 0 & 0 & 0 & 0 \\
0 & 0 & 0 & 0 & 0 & 0 & 0 & 0 & 0 & 1 & 0 & 0 & 0 & 0 & 0 & 0 \\
0 & 0 & 0 & 0 & 0 & 0 & 0 & 0 & 0 & 0 & 1 & 0 & 0 & 0 & 0 & 0 \\
0 & 0 & 0 & 0 & 0 & 0 & 0 & 0 & -\gamma\beta & 0 & 0 & \gamma & 0 & 0 & 0 & 0 \\
-\gamma^2\beta & 0 & 0 & \gamma^2\beta^2 & 0 & 0 & 0 & 0 & 0 & 0 & 0 & 0 & \gamma^2 & 0 & 0 & -\gamma^2\beta \\
0 & -\gamma\beta & 0 & 0 & 0 & 0 & 0 & 0 & 0 & 0 & 0 & 0 & 0 & \gamma & \gamma & 0 \\
0 & 0 & -\gamma\beta & 0 & 0 & 0 & 0 & 0 & 0 & 0 & 0 & 0 & 0 & 0 & 0 & 0 \\
\gamma^2\beta^2 & 0 & 0 & -\gamma^2\beta & 0 & 0 & 0 & 0 & 0 & 0 & 0 & 0 & -\gamma^2\beta & 0 & 0 & \gamma^2
\end{bmatrix}
\times
\begin{bmatrix}
p' - \frac{1}{8\pi} H_x'^2 \\
0 \\
0 \\
0 \\
0 \\
p' + \frac{1}{8\pi} H_x'^2 \\
0 \\
0 \\
0 \\
0 \\
p' + \frac{1}{8\pi} H_x'^2 \\
0 \\
0 \\
0 \\
\eta' c^2 + \frac{1}{8\pi} H_x'^2
\end{bmatrix}
$$

$$
T_{xx} = \gamma^2\left[p' - \frac{1}{8\pi} H_x' + \eta' v^2 + \frac{1}{8\pi} H_x'^2\right. \qquad = -\frac{1}{8\pi} H_x'^2 + \gamma^2[p' + \eta' v^2]
$$

$$
T_{xt} = \gamma^2\left[-\beta p' + \beta \frac{1}{8\pi} H_x'^2 - \eta'\beta - \beta \frac{1}{8\pi} H_x'^2\right] = \gamma^2 c[-\eta' v - \beta/c\, p']
$$

$$
T_{tt} = \gamma^2\left[\beta^2 p' - \beta^2 \frac{1}{8\pi} H_x'^2 + \eta' c^2 + \frac{1}{8\pi} H_x'^2\right] = c^2\left[\frac{1}{8\pi c^2} H_x'^2 + \gamma^2\left(\eta' + \frac{p'\beta^2}{c^2}\right)\right]
$$

Figure 8. Lorentz Transformation of Total Stress-Energy Tensor

reference. These relations are given by

$$\gamma_1^2(\eta_1^1 v_1^2 + p_1) = \gamma_2^2(\eta_2'^2 v_2^2 + p_2)$$

$$\gamma_1^2(\eta_1^1 v_1 + \frac{v_1}{c^2} p_2^1) = \gamma_2^2(\eta_2^1 v_2 + \frac{v_2}{c^2} p_2')$$

$$\gamma_1 \eta_2' v_1 = \gamma_2 \eta_2' v_2$$

where

$$\gamma_i = \frac{1}{\sqrt{1 - v_i^2/c^2}} \qquad \text{relativistic factor}$$

$$i = 1,2$$

$$\eta = \frac{n}{c^2}(mc^2 + E) \qquad \text{Excess energy density over rest energy } mc^2$$

and n is the particle density. Here the primes refer to the frame of reference in which the observer is at rest with respect to the plasma and the unprimed quantities refer to their values in the frame of reference where the observer is at rest with respect to the shock front. The numbers as before refer to the front and the back of the shock. An interesting piont in the derivation is that in the case of parallel shocks, even in the case of a charged fluid, an external magnetic field does not affect the jump relations across the shock front.

The fundamental Hoffmann-Teller treatment is the most suited to study the possibility of shock wave propagation in the streaming electron fluid along a pulsar's magnetic field lines. It is necessary to adapt this formalism to a moving shock front since in their formulation the jump relations are for a stationary shock front.

Jump Conditions for a Moving Shock

In this section we find the jump conditions for a shock wave moving at relativistic velocities in a relativistically streaming plasma. As before the magnetic field will be parallel to the shock wave and so will have no effect on the jump conditions since the velocity vector is parallel to the field vector. The velocities will be in the x direction and v_1 and v_2 will be the velocities of the plasma in front and in back of t the shock as before. In this treatment v will be the velocity of the shock front. To obtain the jump conditions we set up $T_{\mu\nu}$ the total stress energy tensor in the laboratory medium and then Lorentz transform this to the shock front medium exactly as was done by Hoffmann and Teller. This has to be done separately for region 1 and 2 because the front moves with velocities $v + v_1$ and $v - v_2$ in regions 1 and 2 with respect to the stationary lab frame. The lab frame $T_{\mu\nu}$ is just the one used in the stationary shock wave calculation. By a procedure similar to that of Teller we obtain the following jump conditions

$$\frac{\eta_1'(V+v_1)^2 + p_1'}{1 - \frac{(V+v_1)^2}{c^2}} = \frac{\eta_2'(v-v_2)^2 + p_2'}{1 - \frac{(v-v_2)^2}{c^2}} .$$

$$\frac{\eta_1' c(v_1+v) + \frac{(v_1+v)}{c} p_1'}{1 - \frac{(v+v_1)^2}{c^2}} = \frac{\eta_2' c(v-v_2) + \frac{(v-v_2)}{c^2} p_2'}{1 - \frac{(v-v_2)^2}{c^2}}$$

$$\frac{n_1'(v_1+v)}{\sqrt{1-\frac{(v+v_1)^2}{c^2}}} = \frac{n_2'(v-v_2)}{\sqrt{1-\frac{(v-v_2)^2}{c^2}}}$$

These relations demonstrate that shock waves can be formed even if the fluid velocity is very large. The third equation is very interesting. If we assume that the electrons are streaming at high velocities, v_1, v_2 then it is obvious n_2' must be considerably larger than n_1' because

$$\frac{v-v_2}{\sqrt{1-\frac{(v-v_2)^2}{c^2}}} << \frac{v+v_1}{\sqrt{1-\frac{(v+v_1)^2}{c^2}}}$$

thus causing bunching of electrons due to the shock wave. This tendency towards bunching given a discontinuity could be the source of the shocks in the streaming plasma. The parameter of interest here is the thickness of the shock. For the case where it is less than the wavelength of the observed radiation it can produce coherent radiation at all wavelengths longer than this. There have been several treatments of the dimensions of shock fronts. Mott-Smith analyzed the case of a non-ionized gas and found that the thickness was of the order of a few mean free paths of the molecules.[6] Tidmann did a calculation where he treated an ionized gas and found the dimension of the shock front to be given by

$$t = \frac{m^2 v^4}{690\, e^4\, n\, \Lambda},$$

where m and e are the mass and charge of the electron and Λ is the

Coulombic logarithm which is a parameter whose value is close to 40.[7] Substituting values of density 10^{12} cm^{-3} and velocity 3 x 10^{8} cm/s we find that the thickness is of the order of 1 cm. Thickness of this order would be sufficient to explain the coherence of the pulsar radiation. We believe this process can compete effectively with the maser actoon proposed by Cocke and Melrose. In our derivation the viscosity effects have been ignored although the conductivity has not. It cannot be denied, however, that the acoustic speed in the medium itself can be large because the magnetic energy density in free space ($B^2/2u_o$) is about 10^{34} MeV per cubic meter for a B field of 10^{12} G, whereas the rest energy of the electrons (n = 10^{12} cm^{-3}) is approximately 10^{18} MeV per unit volume.

FOOTNOTES

[1]P. A. Sturrock, Astrophys. Jour. 164, 529 (1971).

[2]P. Goldreich and D. A. Keeley, Astrophys. Jour. 170, 463 (1971).

[3]M. A. Rudermann and P. G. Sutherland, Astrophys. Jour. 190, 137 (1974).

[4]V. C. A. Ferraro and C. Plumpton, Introduction to Magneto-Fluid Mechanics, (Oxford University Press, Oxford, 1966).

[5]F. deHoffmann and E. Teller, Phys. Rev. 80, 692 (1950).

[6]H. M. Nott-Smith, Phys. Rev. 82, 885 (1951).

[7]D. A. Tidmann, Phys. Rev. 111, 1439 (1958).

CHAPTER VI

SUMMARY AND CONCLUSIONS

This work started with a short description of the discovery of pulsars and their identification with neutron stars. A survey of the different models for the magnetosphere and the currently subscribed to radiation mechanisms was given. We then made a study of three aspects of the radiation process. The mechanism of radiation by linear acceleration was chosen for its simplicity and its agreement with most magnetosphere models. The spectral and angular distribution of the radiation was calculated numerically using the Lienard-Weichert theory and a fast Fourier transform algorithm. The spectral results compare favorably with observation but the angular distribution appears to be too wide for the currently accepted "forward cone of radiation" models. Lack of agreement is attributed to the unrealistic constant electric field used for accelerating the electrons. The radiative transfer of the signal passing through the magnetosphere was then analyzed. A model was chosen where the plasma in the magnetosphere travels parallel to the star's magnetic field at relativistic velocities and the radiation passes through it making an angle θ with the velocity vector of the plasma. An eighth order polynomial in the index of refraction of the plasma was derived. The cutoff and resonant frequencies of the plasma were calculated and, when the currently accepted values for the particle density, relativistic factor and magnetic field were used, agreed with the observed value.

The contribution of shock waves to the coherence of the radiation was then studied. Following the formalism of deHoffman and Teller the formation of shock fronts due to discontinuities in the supersonic plasma was shown to be possible. Using Tidmann's theory for shock fronts in ionized gases, we found that shocks with thicknesses on the order of the shortest wavelengths observed were possible.

The three main contributions of this work are the calculation of the spectrum of a linearly accelerated charge, the calculation of the plasma cutoff frequency and the relativistic treatment of the dispersion relation, and the calculation of the relativistic shock equations and the thickness of the shock. This work is also the starting point for a number of future works. More realistic accelerating fields may be substituted for the constant electric field in the spectrum calculation in an attempt to get radiation patterns which agree with observation. The expression for the dispersion relation may be solved numerically using currently accepted values for the magnetic field, relativistic factor and charge density. The treatment of plasma waves may be done in the relativistic manner. By studying the transmission of the polarized radiation the value of the magnetic field may be found. This could be related to the height of the plasma through which the radiation traveled. Further work on the formation of shocks in the supersonic plasma flowing along the magnetic field lines is needed. Finally in writing the section on observations the author of this work has noted that a possible explanation for the drifting subpulses is a precession of the neutron star. Neutron stars have long been suspected of being oblate due to their high rotational velocities. If the symmetry axis and rotational axis were not aligned, a precession would occur. This precession could

mean that the times when the radiation from the pulsar swept across our line of sight would shift in a periodic manner. If this is so, it would be important in determining the forces which allow the stars matter to shift in an oblate shape. It would also be of interest to those interested in calculating the gravitational radiation produced by an off-axis rotator and the feasibility of detection of a periodic radiation source.

A SELECTED BIBLIOGRAPHY

Brigham, E. O., The Fast Fourier Transform, (Prentice-Hall, Englewood Cliffs, New Jersey, 1974).

Ginzburg, V. L. and Zheleznyakov, V. V., Ann. Rev. of Astron. and Astrophys. 12, 511 (1975).

Holt, E. H. and Haskell, R. E., Plasma Dynamics, (Macmillan Co., New York, 1965).

Irvin, J. M., Neutron Stars, (Clarendon Press, Oxford, 1978).

Jackson, J. D. D., Classical Electrodynamics, Chapter 14 (John Wiley and Sons, Inc., New York, 1977).

Landau, L. D. and Lifshitz, E. M., The Classical Theory of Fields, (Pergamon Press, New York, 1975).

Manchester, R. N. and Taylor, J. H., Pulsars, (W. H. Freeman and Co., San Francisco, 1977).

Michel, C., Rev. Mod. Phys., 54, 1 (1982).

Smith, F. G., Pulsars, (Cambridge University Press, Cambridge, 1977).

APPENDIX

FUNCTION GENERATION AND THE FAST FOURIER TRANSFORM PROGRAM

The program used to evaluate the transform consists of two sections. The main program reads the parameters: the angle of observation, the limit of integration, and the number of points of the function to be evaluated. It then computes the function between zero and the upper limit of integration, umax, and displays the function if desired. The program then calls a subprogram which computes the Fourier transform of the function. The main program converts the real and imaginary parts to the magnitude and phase and displays the magnitude. Since the integrand is not symmetric the transform will be, with the second half a reflection of the first half of the transform. For this reason only the first half of the transform is displayed.

The use of the fast Fourier transform algorithm calls for some care. The first point deals with discontinuities caused by the truncation of the function to be transformed. Since we must evaluate the function on a finite domain it is necessary to choose a value where the function essentially goes to zero. A sharp discontinuity will add frequency components reflecting it. For this reason the function is displayed so that the user insures that the limit of integration is large enough. It is also important when using the FFT algorithm that the sampling rate is larger than twice the largest frequency of the

signal. This is referred to as the Nyquist criterion. By displaying the function it is evident that our sampling rate is adequate since there is only one peak and the function falls off smoothly. The Nyquist criterion insures us that we miss no structure in the function when sampling it.

The results of the program give us the transform of the function at frequencies which are related to the limit of integration, umax and the number of samples, N. We have the frequency given by the relation

$$\Omega = \frac{n}{umax} \qquad n = 1, N \tag{A-1}$$

This means that the longer the integration time the smaller the frequency increments and the larger the number of samples used the larger the range of frequencies given by the transform. Since the frequency used here is a transformed frequency we must convert back to the actual frequency using the change in variables given by

$$\omega = \frac{a^{+}\Omega}{c} = \frac{e\,E\,n}{m\,c}\,\frac{1}{umax} = 586\,E\,\frac{1}{umax} \tag{A-2}$$

Although the form of the spectrum does not change with electric field strength the frequency range does with the more energetic particles emitting higher frequencies as would be expected.

The program was run once for every 5^{o} from 5^{o} to 180^{o} with the upper limit of integration being adjusted so as to insure that the cut-off value was at least three orders of magnitude lower than the peak value of the function. The running time was about eight minutes for each angle using a 1024 point transform on a 28K PDP 11 microprocessor. The program is given of the next three pages.

```
C     THIS PROGRAM COMPUTES UP TO 2048 SAMPLES OF THE
C     FUNCTION F(U)
C
C     F(U) = SIN4/(A*(A*(1+CSIN2)-2*U*CSIN+2*CSIN2)**2
C
C     WHERE   CSIN = COS(THETA)
C             SIN4 = SIN(THETA)**4
C             CSIN2 = COS(THETA)**2
C             A = SQRT( U**2 - 2*U*CSIN + 1 )
C
C
C     FROM 0 TO SOME SPECIFIED UMAX.  IT THEN CALLS A FFT
C     ROUTINE AND COMPUTES THE FOURIER TRANSFORM OF THE
C     DATA.  THE PROGRAM WILL PRINT THE FUNCTION IF REQUIRED
C     AND THE FIRST HALF OF THE CALCULATED FFT.  ONLY THE
C     AMPLITUDE OF THE TRANSFORM IS PRINTED ALTHOUGH BOTH
C     AMPLITUDE AND PHASE ARE CALCULATED.
      COMMON F
      DIMENSION X(2,2048)
      COMPLEX F(2048)
      EQUIVALENCE (F,X)
      DATA NO/2HNO/
      CALL ASSIGN(2,'KB:')
      CALL ASSIGN(3,'TT:')
999   WRITE(3,1)
1      FORMAT(44H ENTER M, I2, WHERE 2**M = NUMBER OF SAMPLES)
      READ(3,2) M
2     FORMAT(I2)
      N=2**M
      WRITE(2,1000) N
1000  FORMAT(20H NUMBER OF SAMPLES =,I4)
      N1=N/8
      WRITE(3,10)
      READ (3,20) THETA
10    FORMAT(41H ENTER ANGLE OF OBSERVATION, FORMAT F10.5)
20    FORMAT ( F10.5 )
      WRITE(2,2000) THETA
2000  FORMAT(21H OBSERVATION ANGLE = ,F10.5)
      WRITE ( 3,30 )
      READ ( 3,40 ) UMAX
30    FORMAT(39H ENTER MAXIMUM VALUE OF U, FORMAT F10.5)
40    FORMAT (F10.5)
      WRITE(2,3000) UMAX
3000  FORMAT(29H RANGE OF INTEGRATION UMAX = ,F10.5)
      SCALE = UMAX/FLOAT(N)
      DELTU=UMAX/N
      RADIAN = 2*3.14159*THETA/360.
      SINE2 = (SIN(RADIAN))**2
      SINE4 = SINE2**2
      CSIN = COS(RADIAN)
      CSIN2 = CSIN**2
```

```
      DO 70 I=1,N
      RI = (I-1)
      U = RI*DELTU
      A = SQRT(1 - 2.0 * U * CSIN + U*U)
      F(I)=CMPLX(SINE4/(A*(A*(1+CSIN2)-2.*U*CSIN+2.*CSIN2)**2),0.0)
70    CONTINUE
      F(1) = .5 * F(1)
      WRITE(3,71)
71    FORMAT(44H DO YOU WANT THE FUNCTION DISPLAYED, YES/NO?)
      READ (3,72) IANS
72    FORMAT(A2)
      IF (IANS .EQ. NO) GO TO 74
      MAX=0
      DO 73 I=1,N1
      MIN=MAX+1
      MAX=I*8
73    WRITE(2,85) (X(1,L), L=MIN,MAX)
74    ISW = 0
      CALL FFT(F,M,ISW)
      DO 75 I=1,N
      SAVE1 = SCALE * X(1,I)
      SAVE2 = SCALE * X(2,I)
      X(1,I) = SINE2*SQRT(SAVE1**2 + SAVE2**2)
75    X(2,I) = ATAN2(SAVE2,SAVE1)
      WRITE(2,750)
750   FORMAT(1H )
      MAX = 0
      LL = N1/2
      DO 90 J=1,LL
      MIN = MAX+1
      MAX = J * 8
      WRITE(2,85) (X(1,L), L=MIN,MAX)
90    CONTINUE
      REWIND 2
      WRITE(3,100)
100   FORMAT(32H WOULD YOU LIKE TO TRY AGAIN ?     )
      READ(3,72) IANS
      IF(IANS .NE. NO) GO TO 999
85    FORMAT(1P6E15.5)
      CALL CLOSE(2)
      CALL CLOSE(3)
      END
```

```
JC      SUBROUTINE TO CALCULATE THE FAST FOURIER TRANSFORM
C     FROM OPPENHEIMER AND SCHAFER'S BOOK 'DIGITAL SIGNAL
C     PROCESSING', PAGE 332 FIG. P6.5.
C     X IS A COMPLEX ARRAY OF DIMENSION 2048, M IS THE
C     POWER OF 2 WHICH IS EQUAL TO THE NUMBER OF POINTS
C     TO BE TRANSFORMED.  ISW IS THE SWITCH FOR THE
C     TRANSFORM '0' OR THE INVERSE TRANSFORM '1'.
      SUBROUTINE FFT(F,M,ISW)
      ONE=1.
      IF(ISW.EQ.1) ONE=-1
      COMPLEX F(2048), U, W, T
      N=2**M
      PI=3.14159265358979
      DO 20 L=1,M
      LE=2**(M+1-L)
      LE1=LE/2
      U=(1.0,0.0)
      W=CMPLX(COS(PI/FLOAT(LE1)),-ONE*SIN(PI/FLOAT(LE1)))
      DO 20 J=1,LE1
      DO 10 I=J,N,LE
      IP=I+LE1
      T=F(I)+F(IP)
      F(IP)=(F(I)-F(IP))*U
10    F(I)=T
20    U=U*W
      NV2=N/2
      NM1=N-1
      J=1
      DO 30 I=1,NM1
      IF (I.GE.J) GO TO 25
      T=F(J)
      F(J)=F(I)
      F(I)=T
25    K=NV2
26    IF(K.GE.J) GO TO 30
      J=J-K
      K=K/2
      GO TO 26
30    J=J+K
      REALN=N
      IF (ONE.GT.0.0) GO TO 40
      DO 35 I=1,N
35    F(I)=F(I)/REALN
40    RETURN
      END
```

VITA

David James Gordon

Candidate for the Degree of

Doctor of Philosophy

Thesis: A STUDY OF THE RADIATION PROCESS OF PULSARS

Major Field: Physics

Biographical:

Personal Data: Born in Mineola, New York, January 27, 1949, the son of David and Dorothy (Anderson) Gordon.

Education: Graduated from Kingston High School, Kingston, New York, June, 1967; received B. A. degree in physics from Marist College in Poughkeepsie, New York, in May, 1971; obtained New York State Permanent Teaching Certification, February, 1974; was awarded M.A. degree in physics from the State University of New York College at New Paltz, New York, in May, 1974; completed requirements for the Doctor of Philosophy degree in physics at Oklahoma State University, Stillwater, Oklahoma, in July, 1982

Professional Experience: Graduate Teaching Assistant, Physics Department at SUNY College at New Paltz, New York, 1972-1973; Physics Teacher, Franklin D. Roosevelt High School, Poughkeepsie, New York, 1973; Graduate Teaching Assistant, 1974-1981, Research Assistant, 1981-1982, and Lecturer in Physics, 1981-1982 all at Oklahoma State University, Stillwater, Oklahoma; Research Assistant at Phillips Petroleum Research Center in Bartlesville, Oklahoma, Summers of 1975 and 1976; Physics Lecturer, Spartan School of Aviation, Tulsa, Oklahoma, 1978

Professional Organizations: American Physical Society, American Astronomical Society, American Association of Physics Teachers, American Association of Mathematics, and the Society of Exploration Geophysicists.